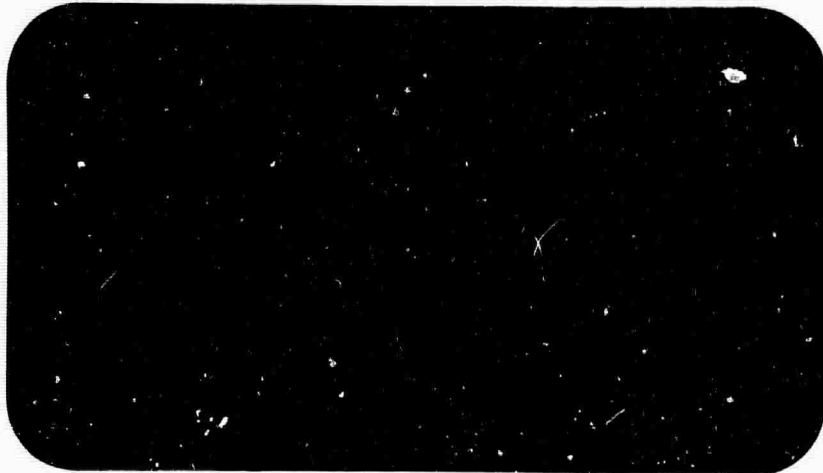


AD 673983

UNIVERSITY OF CALIFORNIA

DEPARTMENT OF PHYSICS



for public use; its distribution is unlimited

AUG 29 1969

LOS ANGELES 24

Reproduced by the
CLEARINGHOUSE
for Federal Scientific & Technical
Information Springfield Va 22151

STUDY OF OPTICAL INTERACTIONS IN SOLIDS

Semiannual Technical Summary Report
(For the Period Ending 31 March, 1968)

Contract: Nonr-233(93)

ARPA Order #306

Principal Investigator: Professor R. Braunstein
University of California at Los Angeles
Los Angeles, California

Starting: September 1, 1966 Expiration Date: August 31, 1968

Issued Date: May 1968

This research is part of Project DEFENDER under the joint sponsorship of the Advanced Projects Agency, the Office of Naval Research, and the Department of Defense.

Reproduction in whole or in part is permitted for any purpose of the United States Government.

Summary:

This is a status report on a program of study of the interaction of intense coherent optical radiation with matter. The following is a summary of the problems investigated during this period:

Multiphoton absorption in semiconductors was investigated with emphasis on the III-V compounds. It was shown that this mechanism can set an intrinsic upper limit to the power density transmittible through semiconductors. This mechanism is an effective means of optically pumping semiconductor lasers, can limit the power density obtainable from such devices, or can enable the fashioning of nonlinear optical elements. Laser action in a large volume of Ga As was excited by double-photon pumping using a Q-switched neodymium laser, yielding output power of the order of a megawatt/cm² at 8365 Å at liquid nitrogen temperature.

A new temperature anomaly of the threshold for stimulated Raman emission in liquid benzene was discovered and investigated. This effect indicates that self-focusing of the exciting laser beam does not explain previously observed Raman thresholds. The following new information is reported:

1. Very strong and critical temperature dependence on the threshold and the gain of the second order stimulated Raman Stokes line at 8,050 Å.
2. New multiphonon stimulated Raman line at 1.07 micron, its line shape and output as a function of laser power.
3. Temperature behavior of the 1.07 micron line.
4. Correlations between the temperature behavior of the preceding stimulated Raman lines.

Preliminary studies of harmonic generation in reflection from piezo-electric metals were begun. There are a number of metals whose point group lacks a center of inversion and consequently have the necessary conditions to be piezo-electric and thus show harmonic generation in reflection. It is shown that the qualitative and quantitative results for these metals will differ from the centro-symmetric metals where second harmonic production is due to $E \cdot \nabla E$ terms.

A technique of derivative spectroscopy was developed which enables the detection of the changes in absorption or reflectivity at levels of one part per million for narrow lines in a continuous-like background. This technique enables the frequency modulation of a spectrometer in any spectral range from the ultra-violet to the far-infrared and to obtain the first and higher derivatives of a line shape. Illustrations of this technique in the study of the singularities in the density of states for optical transitions are reported. This technique of derivative spectroscopy should prove a tool for measuring single and double-photon absorption in gaseous atmospheres.

A new type of gas plasma oscillation is reported, obtained by shunting a He-Ne plasma with an external capacitor. This configuration can work as an oscillator or as a regenerative amplifier.

The feasibility of experimentally observing the reflection of atoms from standing light waves is considered.

Multiphoton Absorption — J. P. Biscar, S. Gratch, R. Braunstein

Calculations have shown that the double-photon absorption cross-sections in a number of semiconductors is sufficiently large to set an intrinsic upper limit to the power density that can be propagated through such media using presently available lasers. In addition, it should be possible to observe double-photon stimulated emission in such systems and so produce difference frequencies by this process. The large cross-sections for this process indicates that double photon absorption is also an effective mechanism for optical pumping of semiconductor lasers, can limit the power density obtainable from such devices, or can enable one to fashion nonlinear optical power limiters.

A direct measure of the two-photon absorption cross-sections in a number of other III-V, II-VI compounds would be extremely valuable to check further aspects of the theory as well as to yield further band structure information not easily obtainable by conventional optical techniques. The desirability of pursuing such studies on the III-V and II-VI compounds is that sufficient band structure information exists for these materials to enable one to predict the two-photon absorption cross-sections with some degree of accuracy. The fact that these compounds have been used as laser sources further dictates the desirability of obtaining these cross-sections, since the power density obtainable from these materials will be limited by this quadratic loss process. In addition, these results can be used for calculating the double-photon stimulated emission cross-sections in the case of a population inversion and so obtain coherent emission or amplification in new regions of the spectrum. For this program, a high power pulsed ruby

and neodymium laser, together with a number of Raman and second harmonic sources were put into operation.

The previous theory, developed for the double-photon absorption in semiconductors utilized a three-band model for the band structures and took into account the parity of the virtual transitions. However, application of this theory to allowed-forbidden two photon absorption in a two-band model, reveals simple generalizations regarding the underlying band parameters which determine the cross-sections for all the III-V and II-VI compounds and so enables one to succinctly set a lower band for this cross-section for this class of materials. The results of this calculation together with the estimates of the cross-sections for selected III-V compounds are given in the Appendix.

Preliminary measurements were made of the two-photon absorption cross-section in GaAs ($E_g=1.51$ eV) using a Q-switched neodymium glass laser ($\hbar\omega=1.17$ eV). The fluorescence excited by the 1.17 eV photons absorbed in GaAs centered at 8365 \AA . The sample of GaAs was a rectangular slab $5 \text{ mm} \times 5 \text{ mm} \times 9 \text{ mm}$ with end surfaces polished flat to form a plane-parallel cavity and was directly immersed in liquid nitrogen. The unfocused laser beam was incident normal to the polished faces and longitudinal to the long direction of the sample. An incident power densities of $50 \text{ megawatts/cm}^2$, the line narrowed to $< 10 \text{ \AA}$ at 8365 \AA and yielded a power output of one megawatt/cm^2 ; this beam seemed to have very little divergence. These manifestations indicated that we were obtaining double-photon pumping and subsequent laser action in GaAs. At these power levels excitation was probably occurring throughout the volume of the sample through which the laser beam was passing. The incident neodymium laser pulse width was $\sim 40 \text{ nsec.}$, while the output pulse at 8365 \AA from GaAs was $< 40 \text{ nsec.}$ wide.

The photoconductivity of the GaAs sample was measured as a function of incident laser intensity and yielded a quadratic dependence of photoconductive signal with incident intensity. This was evidence that a double-photon absorption was the exciting mechanism; this alone is not conclusive evidence for double-photon absorption since the lifetime of the generated carriers can be a function of incident intensity. However, the superlinearity of the fluorescence and evidence of laser action induced by photons of energy $h\nu = 1.17$ eV in a material of $E_g = 1.51$ eV are all good circumstantial evidence for double-photon pumping.

The large length of the sample and the incident power density of ~ 100 megawatts/cm² would have enabled us to check out the nonlinear transmission law (derived in the Appendix) by a direct measurement of the absorption coefficient of photons of $h\nu = 1.17$ eV by GaAs, as a function of intensity. However, it was inconvenient to measure the absorption of the neodymium beam at this time, due to the presence of the intense stimulated frequency at 8365 \AA , for lack of the availability of adequate filtering.

Since the double-photon cross-sections seemed encouragingly large, it was decided to concentrate effort in the direction of trying to observe double-photon stimulated emission at the difference frequency $1.51 \text{ eV} - 1.17 \text{ eV} = 0.34 \text{ eV}$. It was also decided to turn our attention to the use of stimulated Raman lines produced in benzene so as to obtain pairs of convenient lines, one for single quanta primary of GaAs to obtain a population inversion, the other to induce double-photon stimulated emission at the frequency differences between the energy gap and the line below the energy gap.

While this work was in progress an extremely interesting temperature dependent anomaly of the threshold for stimulated Raman in benzene was observed. Since such a temperature anomaly was not previously reported, it was decided to investigate this phenomena in some detail, before returning to the problem of double-photon stimulated emission. The results of the temperature dependent anomaly in benzene will be discussed in the next section.

STIMULATED RAMAN EMISSION IN BENZENE
AND ITS TEMPERATURE BEHAVIOR

J. P. Biscar, S. Gratch, R. Braunstein

Since the discovery of the stimulated Raman effect by Woodbury¹, there has been a rapid increase of investigation as well as an accumulation of puzzles. Some molecules (especially ring-type, like benzene or nitrobenzene) not only show a strong stimulated Raman of the first order, but also a second order effect, and in the case of nitrobenzene, third order. Furthermore, in this case, the intensities of the Stokes and anti-Stokes lines have been found to be equal², in contradiction with the usual approach of energy levels and transition probabilities. The theories of the stimulated Raman effect so far have not satisfactorily explained such other parameters as the Raman gain, the anti-Stokes and Stokes emission angles, the importance of regeneration, and the ratio of forward to backward output.

Finding³⁻⁵ that the gain per unit length in a Raman cell may vary by a factor of five or more, Bloembergen³ explained it by the mode structure of the exciting laser beam. But this was shown not to be the case by F. J. MacDlung, W. C. Wagner, and D. Weiner.⁶ Part of the information of our following data on the intensities of some stimulated Raman lines shows a disturbing, yet precise temperature dependence,

indicating that the gain of the cell may indeed vary by several magnitudes for some lines, for a temperature change as small as 6°C, with all of the other parameters being held constant.

We are also going to discuss the following new informations about the stimulated Raman effect in benzene:

Very strong and anomalous temperature dependence on the threshold and the gain of the second order stimulated Raman Stokes line at 8,050 Å .

New multiphonon stimulated Raman line at 1.07 μ .

Temperature behavior of the 1.07 μ line.

Experimental Conditions

To perform the present research, an unfocused output from a giant pulse ruby laser is used. The dimensions of the ruby crystal are 6" long by 9/16" in diameter. The laser is Q-switched by a rotating prism, providing a two joules pulse with a 25 nanosecond half-width. Inclusion of a sapphire mode selector in the cavity insured a single longitudinal mode output. The cavity is generally 50 cm. long. For the present experiment, we used a diaphragm of 4.2 mm located inside the cavity just in front of the rotating prism.

The Raman cell used in this experiment is 67 cm long, terminated by two optically flat quartz windows. A water jacket surrounding the cell enabled the setting of very precise and stable temperatures. The temperature was varied between 15°C and 40°C. At each temperature setting, a very long time was allowed to elapse so as to attain thermal uniformity throughout the cell. Even at uniform temperatures, the

laser shots were separated by an interval of two minutes for absolute reproducibility (a lot of molecules, broken by the laser filaments, must be removed by dilution). However, the temperature wasn't measured directly inside the benzene, but in the water jacket. There could be a slight difference between these values.

The normal optical setup is shown in Figure 7A for the detection of the 8,050 Å and 1.07 μ lines. The fluorescence of the filters (7-56 or 7-69) was avoided by using part of the beam reflected by a concave glass reflector, which is the equivalent of a neutral density filter of 2.0. Additionally, the dispersion of the quartz prism gave us the possibility of focusing the laser and all of the anti-Stokes lines far from the slit of the monochromator, where the line of interest was focused. This technique improves the performance of the monochromator, which has a scattered light value of 10^{-5} .

The monochromator is a vacuum model Jarrell-Ash and it is absolutely light tight. In the output of the monochromator, we used two different detectors: an RCA 7102 photomultiplier or an SD-100 photodiode (for maximum time resolution). The coupling from the photomultiplier to a 93 ohm cable is made by a transistorized total feedback, high impedance, and low capacitance input element. A Tektronix 547 oscilloscope, triggered by the laser pulse, is used to display the output signal.

To be sure that possible temperature dependent effects on the stimulated Raman lines are not due to some interferential pattern of the cell output, we have been using a large area detector (Photomultiplier 7102) in the configuration shown in Figure 7C, both close to and

far from the output of the cell. The results were the same.

The photodiode has been used, in the configuration shown in Figure 7B, for maximum time resolution.

Threshold of the Stimulated Raman Effect and Self-Focusing

Self-Focusing and Light Trapping

It has been predicted⁷⁻⁸ that a light beam may be trapped at any arbitrary diameter and will thus not spread. Chiao, Garmire, and Townes have further predicted that self-trapping occurs at a critical power level independently of the beam diameter. A photographic picture made by Hauchecorne and Mayer⁹ shows the existence of some high intensity filaments in liquids, but they are generally of very short lifetime.

The existence of a threshold for stimulated Raman, both in the exciting laser intensity and in the length of the liquid cell, was first noted by Eckhardt et al.¹⁰ and subsequently by Stoicheff¹¹. Lallemand and Bloembergen³ measured the Stokes intensity as a function of the cell length at constant laser intensity, and a sharp break indicating the onset of stimulated emission was noted. Bret and Mayer¹² observed that the laser intensity at threshold was a decreasing function of cell length, although such a functional dependence was not explicitly determined.

Self-Focusing and Stimulated Raman Threshold.

Because the stimulated Raman emission occurs only after the beam has traveled some distance through the liquid, it has been proposed¹³ that this is the distance required for self-focusing. This is the

reason that Wang also believes that the threshold of the stimulated Raman is the threshold of self-focusing, and he uses¹⁴ Kelley's equation for the self-focusing length, l :

$$l = \frac{n_0}{4} \left(\frac{a^2}{f} \right) \left(\frac{c}{n_2} \right)^{1/2} \frac{1}{[\sqrt{P} - \sqrt{P_{cr}}]} \quad (1)$$

n_0 : linear index of refraction

c : speed of light

n_2 : related to the dc change in index as defined in reference 7

P : laser input power

P_{cr} : critical power for cylindrical beam trapping.

f : ratio of the radius of the beam, a , to a characteristic radius of curvature of the laser intensity.

To verify such a relation, another criteria for self-focusing other than the stimulated Raman threshold should be used. Certainly, the laser light concentration in filaments is contributing to lower the threshold of the stimulated Raman, but it is not evident that there is an equivalence between self-focusing and the stimulated Raman threshold. On the contrary, our own data indicate that such is not the case.

Benzene Stimulated Raman Line Data

In Benzene it is known that the 992 cm^{-1} and $3,064 \text{ cm}^{-1}$ phonons give stimulated Raman lines at low power threshold, but the Stokes line associated with the $3,064 \text{ cm}^{-1}$ is weak and very broad. On the other hand, the 992 cm^{-1} , for the same power threshold, gives very intense

second order Stokes line at $8,050 \text{ \AA}$. We paid particular attention to this second Stokes line and we studied the temperature dependence of its forward output intensity: The corresponding data are plotted on Figure IA, Figure 2, and Figure 3. Each plot is made at constant incident laser power, respectively 10 MW, 13 MW, and 8.5 MW. Although the shape may change, a minimum was always found around 30°C and a maximum at about 25°C . It is interesting to note that the intensity goes up and down by more than three magnitudes.

A study was made, too, of a new stimulated Raman line at 1.07μ . Its temperature behavior is shown in Figure IB or Figure 4.

Based on the characteristics of the stimulated Raman threshold, we have three main reasons to believe that the self-focusing is not its cause:

1. Two stimulated Raman lines may have two very different threshold powers, all the other parameters being the same.
2. The stimulated Raman threshold may have a temperature dependence impossible to include in the self-focusing equation.
3. The relation $l = \frac{K}{\sqrt{P}}$ from the equation (1) can be directly deduced from the oscillation conditions of a feedback amplifier.

Lines of Different Thresholds

Since the self-trapped light is supposed to reach very high power densities, the threshold of all the stimulated Raman lines in the same liquid should be obtained at the self-focusing threshold. Higher orders of the same optical phonon may have the same threshold, but they are

not independent lines and they may involve the same mechanism. For two independent stimulated Raman lines there is no obvious reason to find the same threshold. We shall now compare the thresholds of the 8,050 Å and the new 1.07 μ stimulated Raman lines of benzene, obtained with the ruby laser. In both cases the same liquid in the same cell (67 cm length) is used with the same laser beam diameter of 4.2 mm. Only the laser power is increased up to the threshold of each line. The threshold of the 8,050 Å (second Stokes of the 992 cm⁻¹ optical phonon; carbon-carbon stretching vibration) can be obtained around 2 Mw, while the 1.07 μ (which involves two times 992 cm⁻¹ plus 3064 cm⁻¹; the latter is the hydrogen-carbon stretching vibration) requires 18 Mw under the same conditions. It's obvious that for the same cell length the threshold of each line depends on the gain of each line. This gain, proportional to the incident laser beam, depends mainly on the mechanisms involved in the particular stimulated Raman line.

Temperature Behavior of the Thresholds

The thresholds of the 8,050 Å line and the 1.07 μ line also depend on the temperature. The gain of each of these lines varies with the temperature. Figure IA shows the relative intensity of the 8,050 Å line vs. temperature for a constant incident laser power of 10 Mw. The output increases by several magnitudes and then decreases again for a small temperature change of 6°C. So, since all of the other parameters are constant, the gain of the molecule for this line changes in the same way, and one can predict from the equation (3) that the

lowest power threshold level of this stimulated Raman line will be where the gain is maximum at a temperature of 25°C, or above 35°C (but in the latter case the stimulated Raman line starts to spread), and the highest laser power threshold level will occur where the gain of the Raman line is minimum.

Self-Focusing and Temperature Behavior

Now consider the self-focusing theory in the same conditions. According to the preceding equation, the cell length we are using, and the critical power of benzene given by Wang, the laser power for the threshold should be around 2 Mw. Although 10 Mw are used in the cell, there is no stimulated Raman line at 15°C and 30°C, and we have no reason to believe that things are different for these two temperatures inside the liquid for self-focusing.

In the Figure IB, the temperature behavior of a new stimulated Raman line at 1.07μ in benzene is shown. One notices that here the amplitude change is relatively small. Furthermore, there are three maxima and they are located at temperatures different from the temperature of the single maximum of the 8,050 Å line.

Since the equation governing the self-focusing should be unique for a given liquid, it is impossible to incorporate the above-mentioned temperature dependence into this equation, because it is so drastically different for the various lines of the same liquid.

It is evident that the common denominator of these two lines is not the self-focusing. The gain and the temperature behavior of each line is very different. Thus, for these feedback oscillators (because of the

stimulation effect), the threshold power, above the critical power, is a function of the wavelength, the temperature, and the length of the cell.

Stimulated Raman Threshold Condition and Feedback Theory

It is interesting to note that a relation like

$$P^{1/2} \propto K \frac{1}{l} \quad (2)$$

verified by Wang¹⁴ in the former equation, can be obtained from the general principles of a feedback oscillator, having a nominal gain G_0 and a feedback β in such a way that the total gain of the feedback amplifier is:

$$G = \frac{G_0}{1 - \beta G_0} \quad (3)$$

For $1 - \beta G_0 > 0$, we have a regenerative amplifier. The Raman cell in this condition can amplify the stimulated Raman emission coming from another source, even if the cell itself cannot generate any stimulated Raman output.

If $1 - \beta G_0 = 0$, then $G_0 = 1/\beta$, and the amplifier becomes an oscillator. In the case of the Raman cell, we have a stimulated Raman output threshold condition.

In a simple approach we can say that the nominal gain G_0 of a Raman cell is proportional to: the laser power, P ; the length of the cell, l ; a function $F(\lambda, T)$, which describes the stimulated Raman behavior of each line at different temperatures; a coefficient A

relating the interaction of the laser beam and the specific liquid. If the absorption coefficient is small, the laser intensity will be constant along the cell and the gain per unit volume will be constant. We can express the gain G_0 of the cell as:

$$G_0 = A \frac{P}{S} \ell F(\lambda, T) \quad (4)$$

Also, the feedback β can be expressed as $\beta = B \ell$, since the probability for a photon to stimulate another one is proportional to the distance it travels in the active medium. Even in single pass feedback, the stimulated Raman in a long cell will be directed along the axis. The threshold condition for the stimulated Raman oscillator becomes:

$$G_0 = \frac{1}{\beta} \Rightarrow A \frac{P}{S} \ell F = \frac{1}{B \ell} \quad (5)$$
$$P^{1/2} = K \frac{1}{\ell}$$

This is verified in reference 14. Extrapolating the graph for an infinite length cell ($1/\ell = 0$), this will give the ordinate for the critical power which could be different for each stimulated Raman line of the same liquid.

Multiphonon Stimulated Raman Line

A new stimulated Raman line has been discovered in benzene at 1.07 μ . Involved in this line are two 992 cm^{-1} phonons and one $3,064\text{ cm}^{-1}$ phonon, with the incident photon wavelength at $6,943\text{ \AA}$.

For a cell 67 cm long, the power threshold is about 130 Mw/cm^2 , meaning that the critical power of this line for an infinite cell could be as high as 100 Mw/cm^2 . Figure 6 shows the line shape at 145 Mw/cm^2 . At 200 Mw/cm^2 (28 Mw with the 4.2 mm diaphragm), an output of approximately 10^4 watts has been estimated, but the line was very broad. Figure 5 shows the relative output power as a function of the laser power. The semi-log plot shows that the output of the line varies exponentially with the incident laser power between 19 Mw and 28 Mw. This is another verification that a stimulated effect is taking place.

Using the SD-100 photodiode (rise time of 2 nanoseconds), the time resolution was limited by the response time of the photodiode and the bandpass of the oscilloscope. However, the 1.07 μ line output pulses looked about ten times sharper than the laser pulse of 25 nanoseconds half-width. Multiple spikes during the laser pulse have been observed, too, and their beginning coincides with the maximum of the laser pulse.

CONCLUSION

The threshold of the stimulated Raman lines should not be used as a criterion of self-focusing. It is sufficient evidence that some short filaments may exist in the Raman liquid and in some cases they can lower the stimulated Raman threshold.

Each stimulated Raman line may have a different critical power, and so different threshold, depending directly on the mechanisms involved inside the molecule for the specific line. At the same time, the same mechanisms involved may show a different temperature behavior. Our interest in this report has been to focus the attention on the molecule itself, suggesting that after the failure of the multi-mode theory and the self-focusing it is the most likely place to find an explanation for most of the strange behavior of the stimulated Raman including the anomalous temperature behavior.

Bibliography

1. E. J. Woodbury, Proc. I. R. E. 50, 2367 (1962).
2. B. P. Stoicheff, "Proc. of International School of Physics - Enrico Fermi," Course XXXI, p. 306, Academic Press, 1964.
3. N. Bloembergen, P. Lallemand, Appl. Phys. Letters 6, 210 (1965).
4. N. Bloembergen, P. Lallemand, Appl. Phys. Letters 6, 212 (1965).
5. N. Bloembergen and Y. R. Shen, Phys. Rev. Letters 13, 720 (1964).
6. F. J. McClung, W. G. Wagner, and D. Weiner, Phys. Rev. Letters 15, 96 (1965).
7. R. Y. Chiao, E. Garmire, and C. H. Townes, Phys. Rev. Letters 13, 479 (1964).
8. G. A. Askarjan, Zh. Eksperim i Teor. Fiz. 42, 1672 (1962)
[translation: Soviet Phys.-J.E.T.P. 15, 1161 (1962)].
9. G. Hauchecorne and G. Mayer, Compt. Rend. 261, 4104 (1965).
10. G. Eckhardt, R. W. Hellwarth, F. J. McClung, S. E. Schwarz,
D. Weiner, and E. J. Woodbury, Phys. Rev. Letters 9, 455 (1962).
11. B. P. Stoicheff, Phys. Letters 7, 186 (1963).
12. G. Bret and G. Mayer, Proc. of the Phys. of Quantum Electronics
Conf., p. 180 (McGraw-Hill, 1966).
13. P. L. Kelley, Phys. Rev. Letters 15, 1005 (1965).
14. C. C. Wang, Phys. Rev. Letters 16, 344 (1966).

Figure Captions

- Fig. 1: Plot of the relative output intensity of the 8,050 Å and the 1.07 stimulated Raman lines vs. temperature at constant laser power density. The Raman liquid is benzene. The cell length is 67 cm. (Beam diameter is 4.2 mm.)
- Fig. 2: Plot of the intensity of the 8,050 Å line vs. temperature for a 13 Mw incident laser power. (Beam diameter is 4.2 mm.)
- Fig. 3: The same as Fig. 2 except that the laser power is 8.5 Mw. (Beam diameter is 4.2 mm.)
- Fig. 4: Plot of the output intensity of the 1.07 stimulated Raman line vs. temperature at a laser power of 19.5 Mw, just above the threshold. (Beam diameter is 4.2 mm.)
- Fig. 5: Logarithmic plot of the relative output power of the stimulated Raman line at 1.07 as a function of the incident laser power. The Raman active liquid is benzene. The Raman cell is 67 cm long. The laser beam diameter used is 4.2 mm.
- Fig. 7: Schematic diagram of the optical setup for the observation of the stimulated Raman lines.

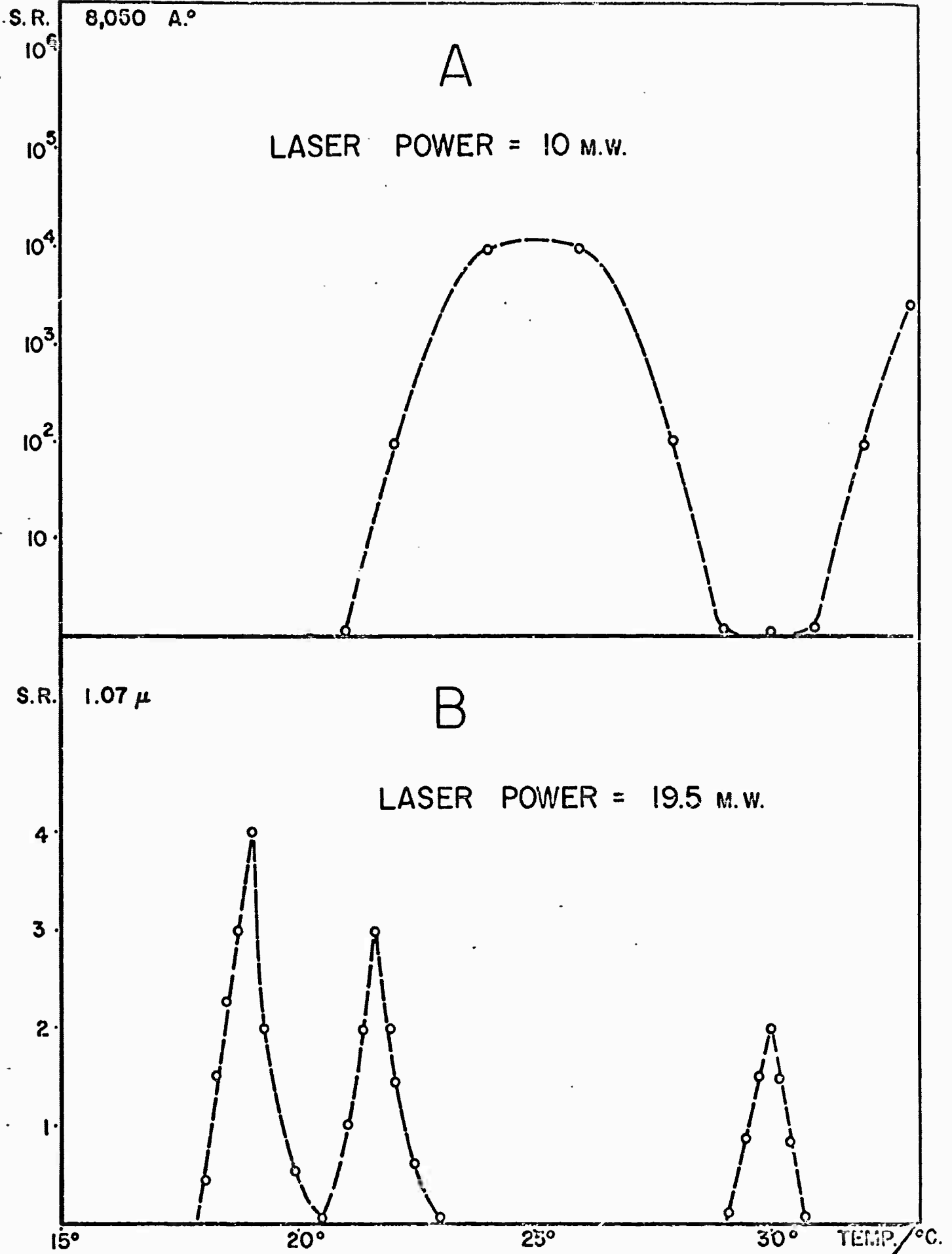


FIG. 1

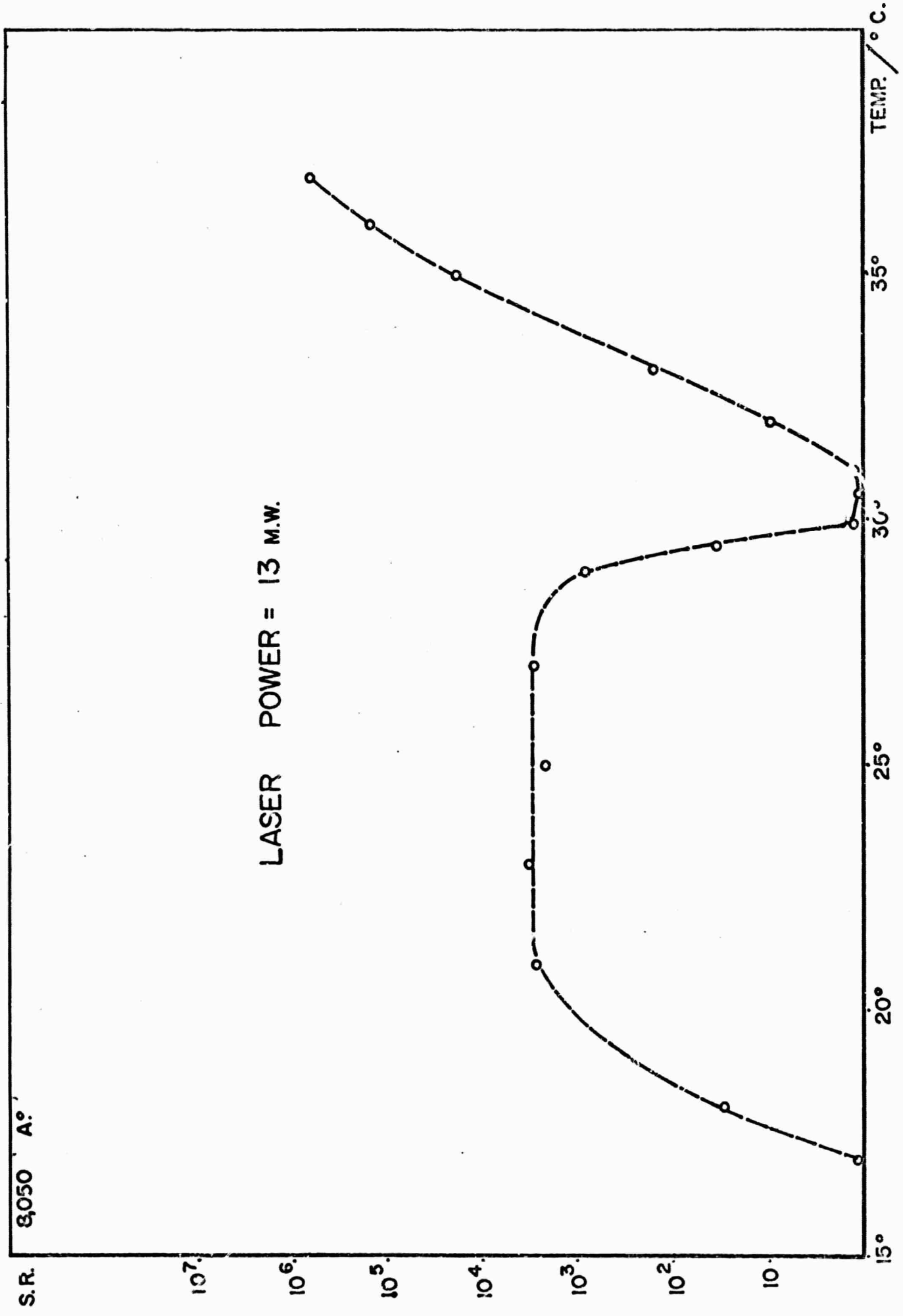


FIG. 2

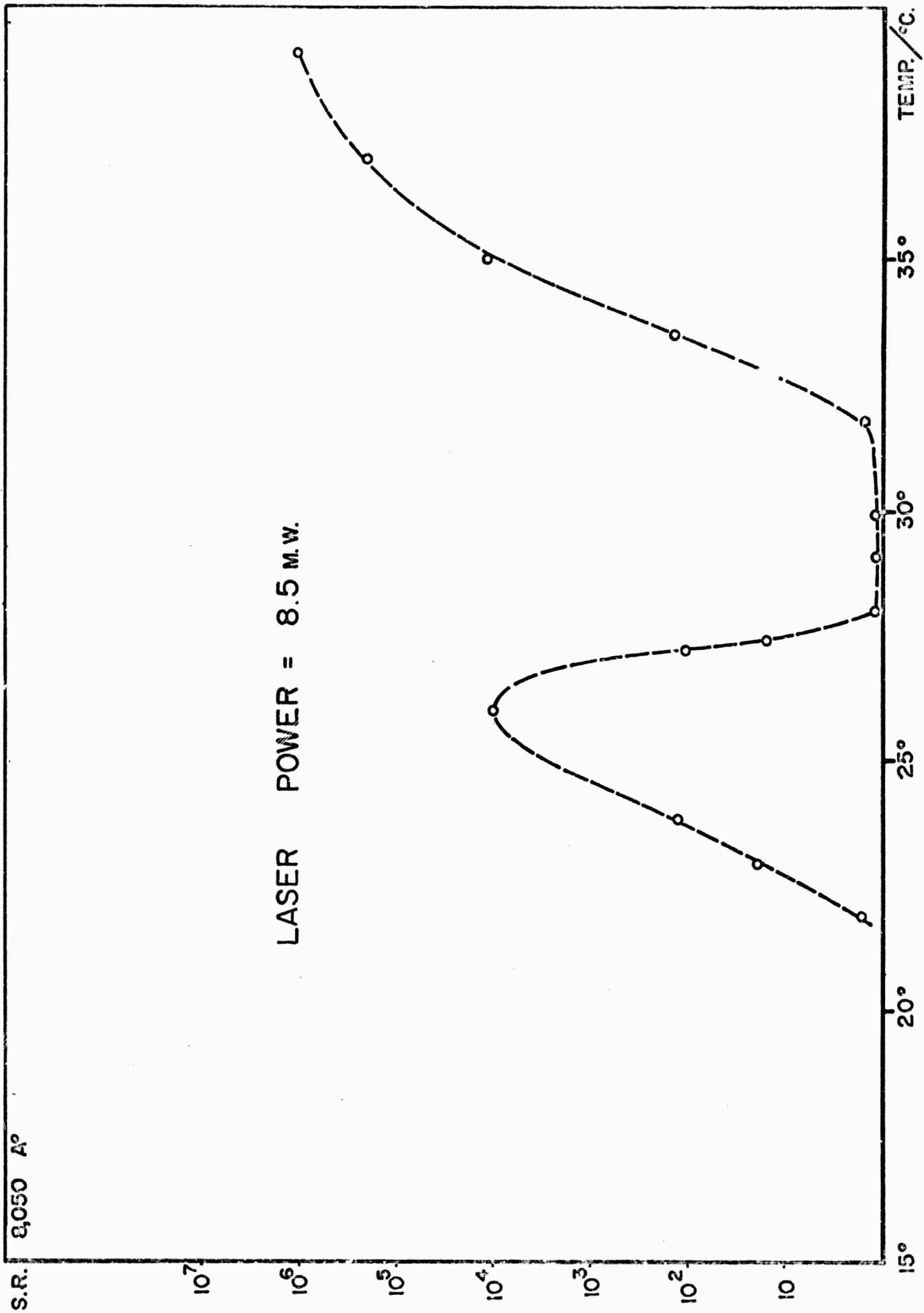


FIG. 3

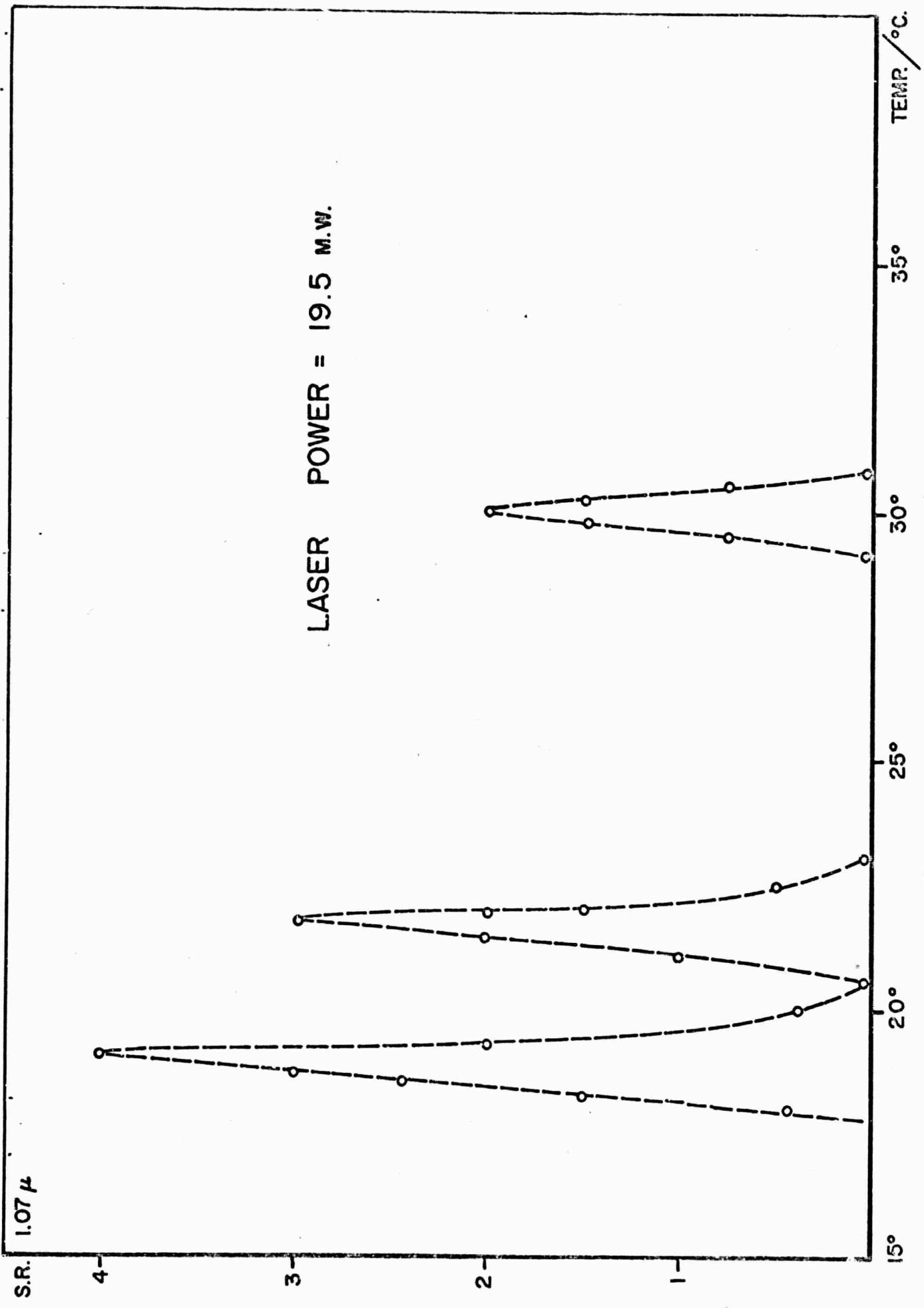


FIG. 4

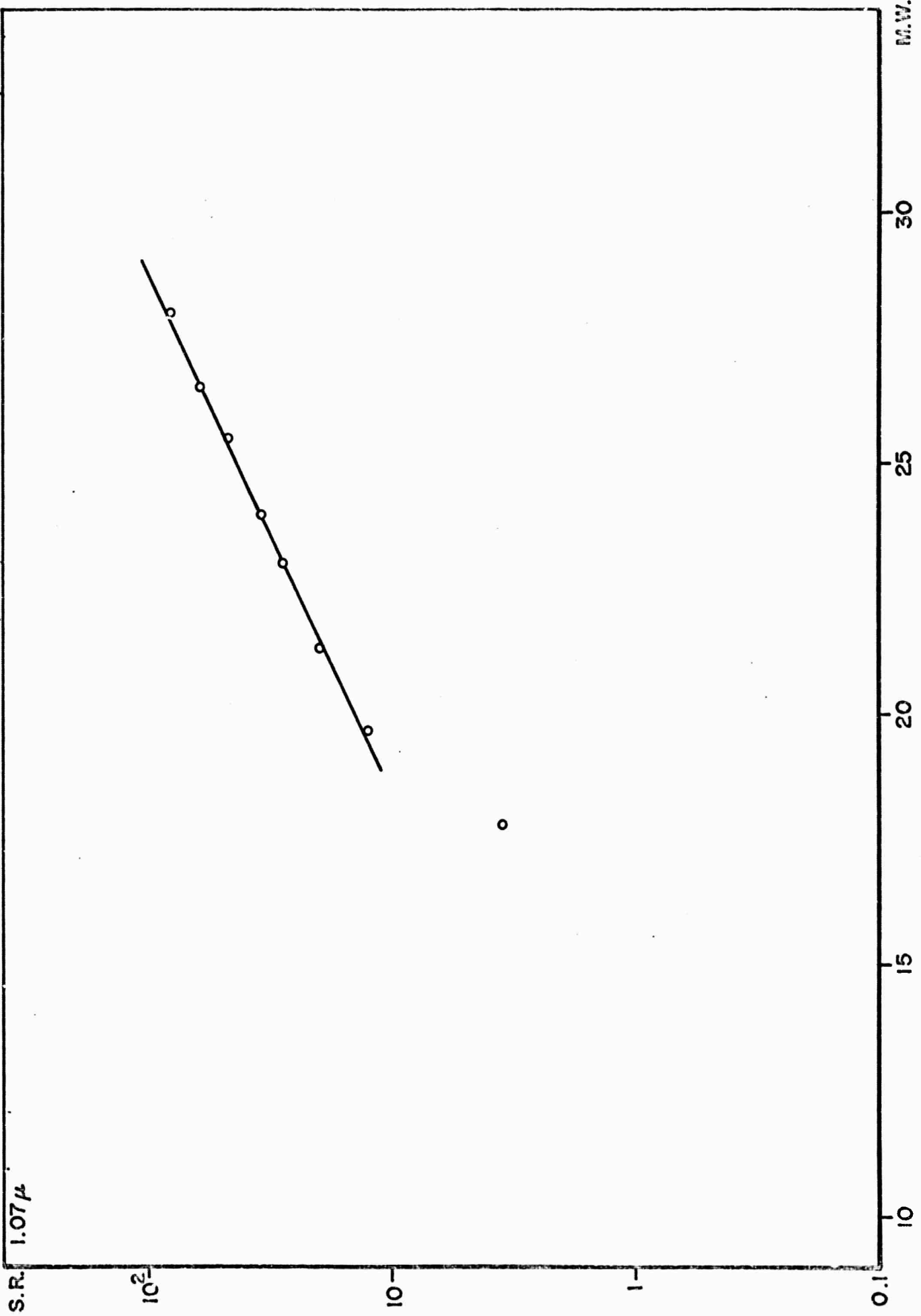


FIG. 5

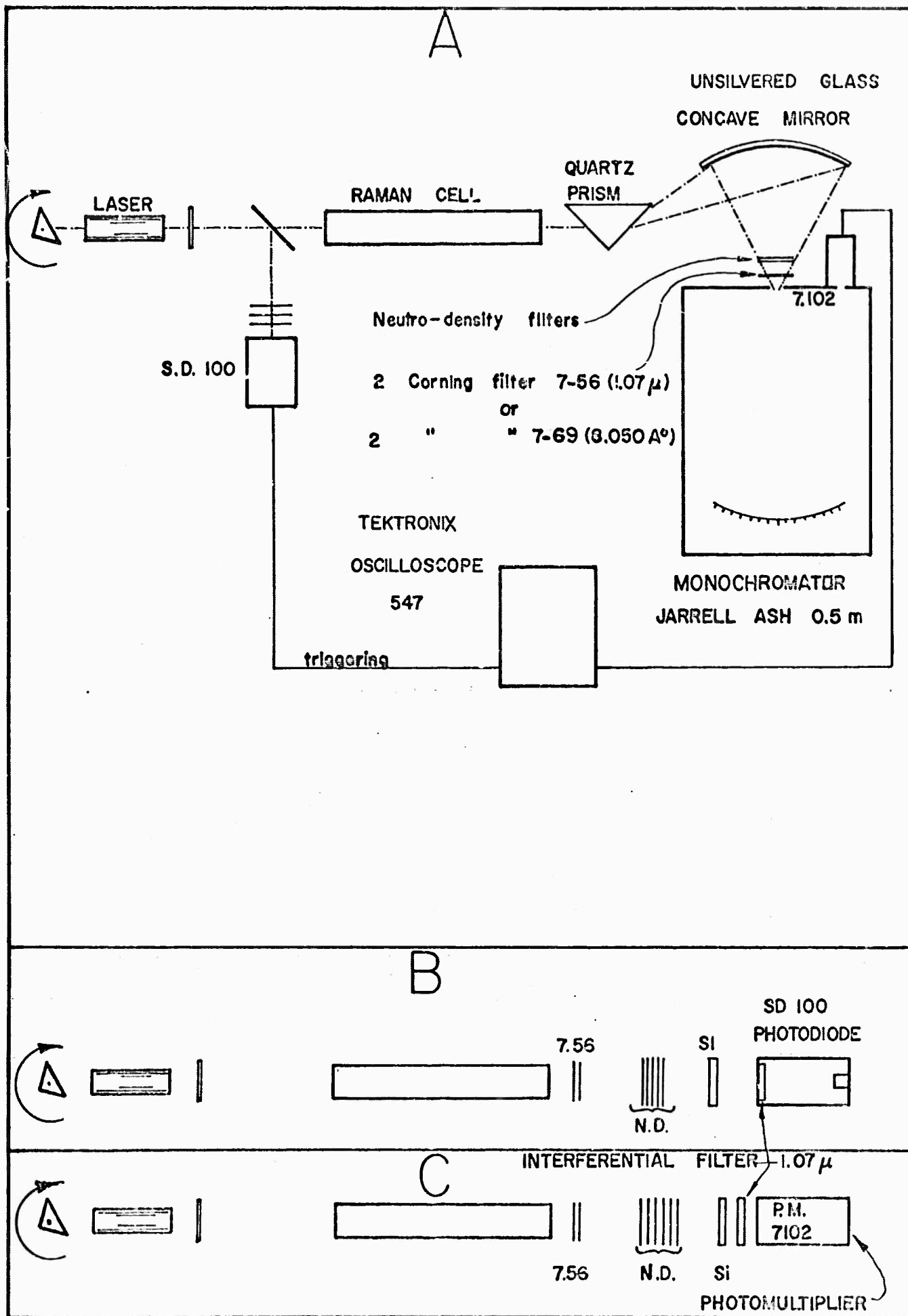


FIG. 7

GENERATION OF HARMONICS IN REFLECTION FROM PIEZO-ELECTRIC METALS

S. Gratch and R. Braunstein

There are a number of metals whose point group lacks a center of inversion and consequently have the necessary condition to be piezo-electric. However, it would be quite impossible to determine the piezo-electric coefficients by conventional dc means because of the large metallic conductivity. A measurement of the nonlinear susceptibility by observing the second harmonic produced by laser beam in reflection would yield the desired coefficients. The results would be of particular interest in determining electron-phonon interactions of these metals. The qualitative and quantitative results for the piezo-electric metals will differ from the centrosymmetric metals where second harmonic production presumably takes place from a single atomic layer, due to the $E \cdot VE$ term. Of all the monatomic metals the α -phase of manganese is the only one that has a point group $43m$ and so can be piezo-electric.

It is possible to generate a harmonic frequency of an incoming beam in reflection from the surface of a medium. For generation in the bulk of a crystal, it is necessary that the crystal lack inversion symmetry. The harmonic generation in reflection may be due to several mechanisms. It may be due to the non-linear polarization produced in the bulk of the material;^{1,2} that produced in the plasma contained in the crystal,³ or that produced in the surface atoms⁴. It can be shown quite generally,¹ that the harmonic will propagate parallel to the reflected fundamental. Let $k_x^R(2\omega)$ be the component of the wave vector of the reflected harmonic perpendicular to the

normal. Then

$$\sin \theta_R (2\omega) = \frac{k_x^R (2\omega)}{|k^R (2\omega)|} \quad (1)$$

The absolute values of the wave vector are determined from

$$|k (\omega_i)| = \epsilon^{1/2}(\omega) \frac{\omega_i}{c} \quad (2)$$

where $\epsilon(\omega_i)$ is the dielectric constant of the medium, in this case air, at the frequency ω_i . The boundary condition leads to

$$k_x^R (2\omega) = 2 k_\alpha^I (\omega) \quad (3)$$

where $k_\alpha^I (\omega)$ is the perpendicular component of the wave vector of the fundamental, and so

$$\sin \theta_R (2\omega) = \frac{2 k_\alpha^I (\omega)}{\epsilon(2\omega) \frac{2\omega}{c}} = \frac{k^I (\omega)}{\epsilon(\omega) \frac{\omega}{c}} = \sin \theta_I^I (\omega) = \sin \theta_R (\omega) \quad (4)$$

The first of these possibilities, a nonlinear polarization produced in the bulk, is a sensitive function of the orientation of the polarization of the incoming fundamental beam relative to the crystallographic axes. The polarization of the harmonic will reflect this sensitivity. To see this in detail, let us use the treatment of Bloembergen and Pershan¹. We first introduce a nonlinear source

$$\underline{P}^{nls} (2\omega) = \underline{\chi} (2\omega) : \underline{E} (\omega) \underline{E} (\omega) e^{2i [k^T (\omega) \cdot \underline{r} - \omega t]} \quad (5)$$

The electric field just inside the surface is related to the incident electric field, $\underline{E}^I(\omega)$, by the Fresnel relations. The electric field amplitude of the reflected harmonic can be resolved into a component perpendicular to the surface, E_{\perp}^R , and one parallel to the surface E_{\parallel}^R , which are found to be

$$E_{\perp}^R = P_{\perp}^{nls} f_1 \left[\theta_I(\omega), \epsilon_m(\omega), \epsilon_m(2\omega), \epsilon(\omega), \epsilon(2\omega) \right] \quad (6a)$$

$$E_{\parallel}^R = P_{\parallel}^{nls} f_2 \left[\theta_I(\omega), \epsilon_m(\omega), \epsilon_m(2\omega), \epsilon(\omega), \epsilon(2\omega) \right] \quad (6b)$$

with f_1 and f_2 being functions of the dielectric constants of the material from whose surface the harmonic is being generated, the dielectric constant of the medium containing the incoming and reflected beams and the angle of incidence of the fundamental beam. Assuming a cubic or isotropic crystal, the crystallographic orientation will contribute only to the fundamental beam. Assuming a cubic or isotropic crystal, the crystallographic orientation will contribute only to $\underline{p}^{nls}(2\omega)$.

As an example, let us consider a crystal with symmetry 43m, such as GaAs or α - Mn. Here, the only non-vanishing components of $\chi(2\omega)$ are $\chi_{xyz}^{(2\omega)}$, $\chi_{zxy}^{(2\omega)}$, and $\chi_{yzx}^{(2\omega)}$, these are equal to the same value χ .

If we take the normal of the surface as the $[0, \bar{1}, 0]$ direction, the angle of incidence is 45° , and the polarization of the fundamental normal to the plane of incidence and at an angle ψ to the $[001]$ direction then we have from (5)

$$P_{\perp}^{m\ell s}(2\omega) = \frac{3}{2} \chi E^2(\omega) \sin^2 \phi \cos \phi \quad (7a)$$

$$P_{\parallel}^{m\ell s}(2\omega) = \frac{1}{2} \chi E^2(\omega) \sin \phi (1 - 3 \cos^2 \phi) \quad (7b)$$

The harmonic produced by the latter two effects, is, as opposed to that produced due to the bulk properties, insensitive to the crystallographic orientations. On the other hand it is highly sensitive to the angle of the polarization of the fundamental to the plane of incidence. The electron plasma contribution has been treated theoretically^{3,5,6} and this treatment⁶ of the ratio of the intensity of the reflected harmonic to the fundamental yields for an angle of incidence of 45° in the limit of the plasma frequency $\omega_p^2 = \frac{4\pi n e^2}{m}$ being much larger than the square of the fundamental frequency

$$R = \left(\frac{e E_{inc}}{m \omega_p c \mu} \right)^2 \left[48 \cos^4 \Theta - \cos^2 \Theta \sin^2 \Theta + 4 \sin^4 \Theta \right] \quad (8)$$

where:

$$\Theta = \angle \text{Polarization of fundamental to plane of incidence} \quad (9a)$$

$$\mu = \frac{\omega_p}{\omega} \approx 6 \text{ FOR } M_N - \alpha \quad (9b)$$

Experimental evidence seems, on the one hand, to lead one to believe that the plasma effects are dominant⁷ and on the other hand, that the surface effect⁸ is dominant. For the latter, it is necessary that the incident electric field have a component parallel to the plane of incidence and perpendicular to the surface.

For the specific case of Mn- α what then is the prospect of experimentally observing the harmonic in reflection due to the bulk properties. The materials constants need to estimate the magnitude of the effects are unavailable. From the data on optical constants of several metals⁹ and the Fresnel equation for polarization perpendicular to the plane of incidence, and an angle of incidence of 45°

$$E(\omega) \approx \frac{2 E_{inc}}{1 + 0.4 i} \quad (10)$$

If one uses the self constant values for the dielectric constants⁵ in the approximation that ϵ is predominately the electron plasma which is determining the optical electric properties, the expressions in (6a) and (6b) become for $\mu^2 \gg 1$

$$E_{\perp}^R \approx \frac{16 \pi P_{\perp}^{mes}}{5 \mu^2} \quad (11a)$$

$$E_{\parallel}^R \approx - \frac{16 \pi P_{\parallel}^{mes}}{\mu^2 (2+i)} \quad (11b)$$

For a single crystal, it is clear that the contribution of the bulk properties, should be identifiable by the crystallographic orientation. The surface atom contribution will be absent for polarization parallel to the surface. The plasma contribution should be very much smaller than the bulk effect if one assumes $\chi \approx 10^{-6}$.

For a polycrystalline sample, calculations have yet to be carried out to ascertain the dependence on the angle θ , but it is felt that because of the factors mentioned above, the bulk effect should be much stronger.

At the present time instrumentation is being developed to look for the effect. As a test of the experimental arrangement we will do the harmonic generation in some semiconductors, GaAs, Ge and Si and also some metals, Ag, Al and Au.

Initially the monatomic metal α -manganese is being investigated. If this investigation proves promising, the study will be extended to other binary and ternary metals whose point group is $\bar{4}3m$ and so can be piezoelectric.

REFERENCES

1. N. Bloembergen and P. S. Pershan, "Light Waves at the Boundary of Nonlinear Media," Phys. Rev. 128, 606 (1962).
2. J. A. Armstrong, N. Bloembergen, J. Ducuing and P. S. Pershan, "Interactions Between Light Waves in a Nonlinear Dielectric," Phys. Rev. 127, 1918, (1962).
3. Sudhanshu S. Jha, "Theory of Optical Harmonic Generation at a Metal Surface," Phys. Rev. 140, A2026 (1965).
4. P. A. Franken and J. F. Ward, "Optical Harmonics and Nonlinear Phenomena," Rev. Mod. Phys. 35, 23 (1963).
5. N. Bloembergen and Y. R. Shen, "Optical Nonlinearities of a Plasma," Phys. Rev. 141, 298 (1966).
6. Sudhanshu S. Jha, "Nonlinear Optical Reflection from a Metal Surface," Phys. Rev. Letters 15, 412 (1965).
7. Fielding Brown, Robert E. Parks and Arthur M. Sleeper, "Nonlinear Optical Reflection from a Metallic Boundary," Phys. Rev. Letters 14, 1079 (1965). (See also Fielding Brown and Robert E. Parks, "Magnetic-Dipole Contribution to Optical Harmonics in Silver," Ibid. 16, 507 (1966).
8. N. Bloembergen, R. K. Chang and C. H. Lee, "Second Harmonic Generation of Light in Reflection from Media with Inversion Symmetry," Phys. Rev. Letters 16, 986 (1966).
9. L. G. Schultz, "The Optical Constants of Silver, Gold Copper and Aluminum, I. "The Absorption Coefficient $\pm k$," J. Opt. Soc. America 44, 357 (1954) and L. G. Schultz and F. R. Tangheslini, "Optical Constants of Silver, Gold, Copper and Aluminum." II. "The Index of Refractions," Ibid. 55, 362 (1954).

DERIVATIVE SPECTROSCOPY

P. Schrieber, M. Welkowsky and R. Braunstein

There are a number of applications for which it is desirable to sweep the frequency of a monochromator at relatively rapid rates. In the case of signal averaging using multi-channel analyzer techniques for detecting weak spontaneous Raman lines, the signal to noise is enhanced proportional to the square root of the number of sweeps through the line. In order to detect very weak narrow absorption lines out of a background of relatively smooth absorption, it would be desirable to obtain the derivative of the absorption since conventional techniques require a highly stable optical detecting system. We have developed a technique which enables us to frequency modulate a spectrometer in any desired spectral range. This technique has rather wide applicability in a number of areas. Since there has been a number of developments in derivative techniques for the study of band structure of solids, we shall describe the present technique in some detail in the context of band structure studies. However, the same methods can be used to measure small narrow absorption bands in liquids and gases.

During the past few years, several new techniques¹⁻⁷ have been developed which have made it possible to determine the singularities in the density of states for optical transitions in solids. These techniques are essentially derivative techniques which allow the detection of very small changes in optical absorption or reflectivity in an otherwise flat background. The common denominator of all these techniques is that some material parameter is modulated and the derivatives of the corresponding optical absorption or reflectivity

is measured by a phase sensitive detector. The advantage of these new techniques is that they give rise to large effects at critical points such as band edges or saddle points, resulting in converting otherwise continuous-like spectra into line-like spectra with the consequent ease in measuring the positions of these singularities. The electro-optical technique¹⁻⁵ may be used on insulators and semi-conductors, while the piezo-optical^{6,7} technique may be used for insulators or metals. The recently developed thermal-derivative technique can be used on most materials.⁸ However, all these methods are necessarily restrictive in their applicability since they require appropriate sample preparation to which stress, electric fields, or thermal rise in temperature is to be applied. In addition, all these techniques yield line shapes which are not completely understood.

It would be desirable in this field to have a method of obtaining the derivative of the absorption or reflectivity as a function of wavelength without recourse to the actual modulation of the optical properties of the material. In this manner, it would then be possible to locate the singularities and then to separately study the effects of stress, electric fields, or temperature. Essentially, what is needed is a frequency modulated spectrometer, so that appropriate phase sensitive of the detection signal would yield first or higher derivatives. We have developed such means of frequency modulation anywhere from the ultra-violet to the far-infrared at depths of modulation of $\frac{\Delta\lambda}{\lambda} \approx 10^{-3}$ at frequency rates up to a kilocycle/sec. We have demonstrated that such a device is capable of measuring changes in absorption or reflectivity at levels of one part per million for narrow lines out of a continuous background.

Several methods have been reported for producing derivative spectra.⁹⁻¹³ In one class,^{9,10} differentiation is obtained by electrical differentiation of the output signal with respect to time in an analogue fashion. This method has the disadvantage that the value of the derivative is a function of the scanning speed. However, differentiating the independent variable, such as the wavelength, is not subject to this disadvantage. The wavelength of a spectrometer may be modulated by varying the wavelength of the light incident on the detector. This may be done by the vibration of one of the slits^{11,13} or by oscillating the deflection of the beam through the exit-slit by the use of a refractor plate.¹² Both of these methods require a modification of the spectrometer and in addition, the latter is limited by the transmission characteristics of the refractor plate. A more universal method which requires a minimum of interference with an existing spectrometer and requires very little auxiliary equipment is to oscillate a deflecting mirror within the spectrometer.

Figure 1 shows the experimental arrangement for obtaining the derivative of an optical quantity. The only modification within the spectrometer is an additional structure upon which the exit mirror is mounted which enables it to be oscillated at a frequency and amplitude determined by the voltage applied to a piezo-electric element connected in a bimorph configuration. The mounting of the exit-slit diagonal mirror in Perkin-Elmer 99G, 210 and 301 monochromators was so modified the frequency of oscillation of the mirror can be from 30/1000 cycles/sec. and yield an amplitude of oscillation so that the depth of modulation was at $\frac{\Delta\lambda}{\lambda} \approx 10^{-3}$ in the wavelength range 3000Å-20,000Å.

The intensity of the light falling on the detector after transmission through a sample is given by:

$$I(\lambda) = \frac{[1-R(\lambda)]^2 \exp[-K(\lambda)d]}{1-R^2(\lambda) \exp[-2K(\lambda)d]} \cdot I_0(\lambda) \quad (1)$$

where K , R and d are the absorption coefficient, reflectivity and thickness of the sample and $I_0(\lambda)$ is the incident intensity on the sample. In regions where the transmission is not too great, i.e., $K(\lambda)d > 1$, we can let the denominator equal unity and:

$$I(\lambda) = (1-R)^2 \exp[-K(\lambda)d] I_0(\lambda) \quad (2)$$

If we neglect the spectral dependence of R

$$\frac{dI}{d\lambda} = (1-R)^2 \frac{dI_0}{d\lambda} e^{-K(\lambda)d} - \frac{dK(\lambda)}{d\lambda} (1-R)^2 d I_0 e^{-K(\lambda)d} \quad (3)$$

If the slits of the monochromator are adjusted so as to keep the light intensity falling on the detector a constant, we obtain:

$$\frac{\frac{dI(\lambda)}{d\lambda}}{I} = \frac{\frac{dI_0(\lambda)}{d\lambda}}{I_0} - \frac{dK(\lambda)}{d\lambda} \cdot d \quad (4)$$

Thus we see if the contribution to $\frac{dI(\lambda)}{d\lambda} / I$ from atmospheric absorption, the wavelength response of the detector, and the light source is small compared to that of the sample, it is possible to obtain the derivative of the absorption coefficient with respect to wavelength. If the contribution from the source background is

comparable to that of the sample, a separate run without the sample will yield $\frac{dI_c}{d\lambda} / I_c$ and the derivative of the absorption coefficient can be calculated. A separate run to obtain the background derivative can be obviated by the use of a double-beam optical system such as the Perkin-Elmer 301 where the derivative of the signal through the sample and that of the background are simultaneously measured and the background correction made by an electric analogue circuit.

It should be noted that by this method of direct differentiation, i.e., by frequency modulating the macrochromater, the line shapes at the singular points are obtained unambiguously. This is in contrast to the electro-optical piezo-optical, or thermo-optical technique where a material parameter is modulated and so the observed line shape of the derivative must be unfolded from the raw data by theoretical considerations.

The experimental arrangement for obtaining the derivative of a spectra is shown in Figure 1. The light signal incident on the sample is amplitude modulated at 13 c.p.s. by a chopping wheel and the rectified d.c. component is fed to a servo control which adjusts the slits of the monochromater to keep a constant incident intensity on the detector so as to maintain a fixed d.c. operating point on the detector. The exit-slit mirror is driven at ~ 200 c.p.s. and this a.c. component of the transmitted beam is detected synchronously with the voltage driving the piezo-electric bimorph. The frequency of oscillation is chosen as high as possible to overcome the $1/f$ noise in the detecting system. The frequency of modulation depends upon the mass resonance frequency of the mirror system. Although maximum amplitude occurs at 200 c.p.s. frequencies up to 1000 c.p.s. can be obtained with somewhat decreased modulation.

In order to demonstrate the operation of the derivative spectrometer, the following data was taken using the green-line of a Hg-arc as the source. A Perkin-Elmer 210 monochromator was used, with an RCA 1P28 Photomultiplier as the detector, in conjunction with a PAR HR-8 lock-in-amplifier. Figure 2a shows the amplitude of the green line, Figure 2b and Figure 2c show the first and second derivative of this line at a modulation voltage which did not cause any appreciable broadening of the line. Figures 2b and 2c also show the same sequence of data taken with larger modulating voltage where the line widths of the derivative spectra are modulation broadening caused by the fact that the depth of frequency modulation is comparable with the instrumental line width.

Phonon-assisted indirect transitions in transmission and the singularities in the reflectivity of semiconductors were investigated using the above techniques. Figure 3 shows the phonon-assisted indirect transitions in silicon at room temperatures. This figure shows the actual chart recording of both the derivative of silicon and the derivative of the background I_0 . One should note the small structure in the $\frac{dI_c}{d\nu}$ signal. The net result of interest, $\frac{dK}{d\nu}$, is derived by taking the difference of these two signals, but as the $\frac{dI_0}{d\nu}$ signal is roughly constant, the main structure of is apparent in the $\frac{dI}{d\nu}$ signal.

The plasma edges of the noble metals silver and gold have been investigated using this method in reflection and transmission using aluminum as a standard. Figure 4 shows the derivative of the reflectivity of silver in the region of the plasma absorption. In this region the derivative of the aluminum reflectivity is practically flat so that this figure represents the net result $\frac{dR}{d\nu}$.

Although in this report we have illustrated the use of derivative spectroscopy in emission, transmission and reflection in solids, it was possible to detect very weak atmospheric absorption in moderately short laboratory paths by this technique. This derivative technique should prove very useful in measuring single and double-photon absorption in gases and solids.

REFERENCES

1. B. O. Seraphin and N. Bottka, Phys. Rev. Letters 15, 104 (1965).
2. B. O. Seraphin, Phys. Rev. 140, A1716 (1965).
3. B. O. Seraphin and N. Bottka, Phys. Rev. 145, 628 (1966).
4. K. L. Shaklee, F. H. Pollak and M. Cardona, Phys. Rev. Letters 15, 883 (1965).
5. A. Frova, P. Handler, F. A. Germano and D. E. Aspnes, Phys. Rev. 145, 575 (1966).
6. M. Garfinkel, J. J. Tiemann and M. E. Engeler, Phys. Rev. 148, 695 (1966).
7. M. E. Engeler, M. Garfinkel and J. J. Tiemann Phys. Rev. Letters 16, 239 (1966).
8. J. Feinleib, W. J. Scouler and J. Hanus, Bull. Am. Soc. 12, 347, (1967).
9. Edward C. Olson and Clayton D. Alway, Analytical Chemistry 32, 370 (1960).
10. G. I. Collier and F. Singleton, J. Appl. Chem. 6, 495 (1956).
11. C. S. French and A. B. Church "Annual Report of Carnegie Institution of Washington", p. 162 (1954-5).
12. I. G. McWilliam, Journ. of Scientific Instruments 36, 51 (1959).
13. I. Balslev, Phys. Rev. 143, 636 (1966).

FIGURE CAPTIONS

1. Schematic diagram of optical set-up used to obtain the derivation of a spectrum.
2. Emission of the green-line of H_g , together with the first and second derivative. Also are shown the same spectra taken under conditions where the depth of modulation is comparable to the instrumental line width showing the effects of modulation broadening.
3. Derivative of the phonon-assisted indirect transitions in silicon at room temperatures.
4. Derivative of the plasma edge of silver in reflection.

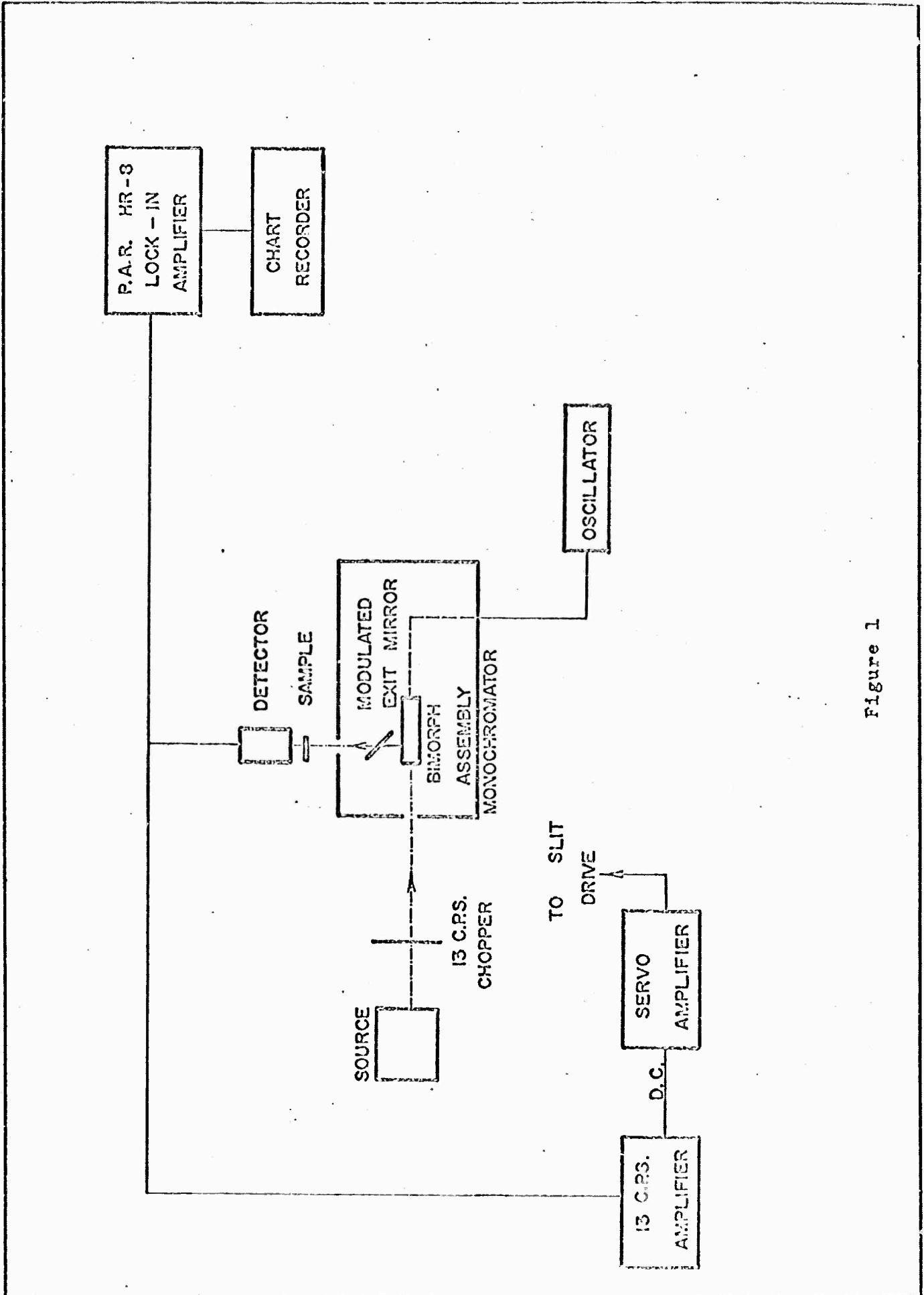
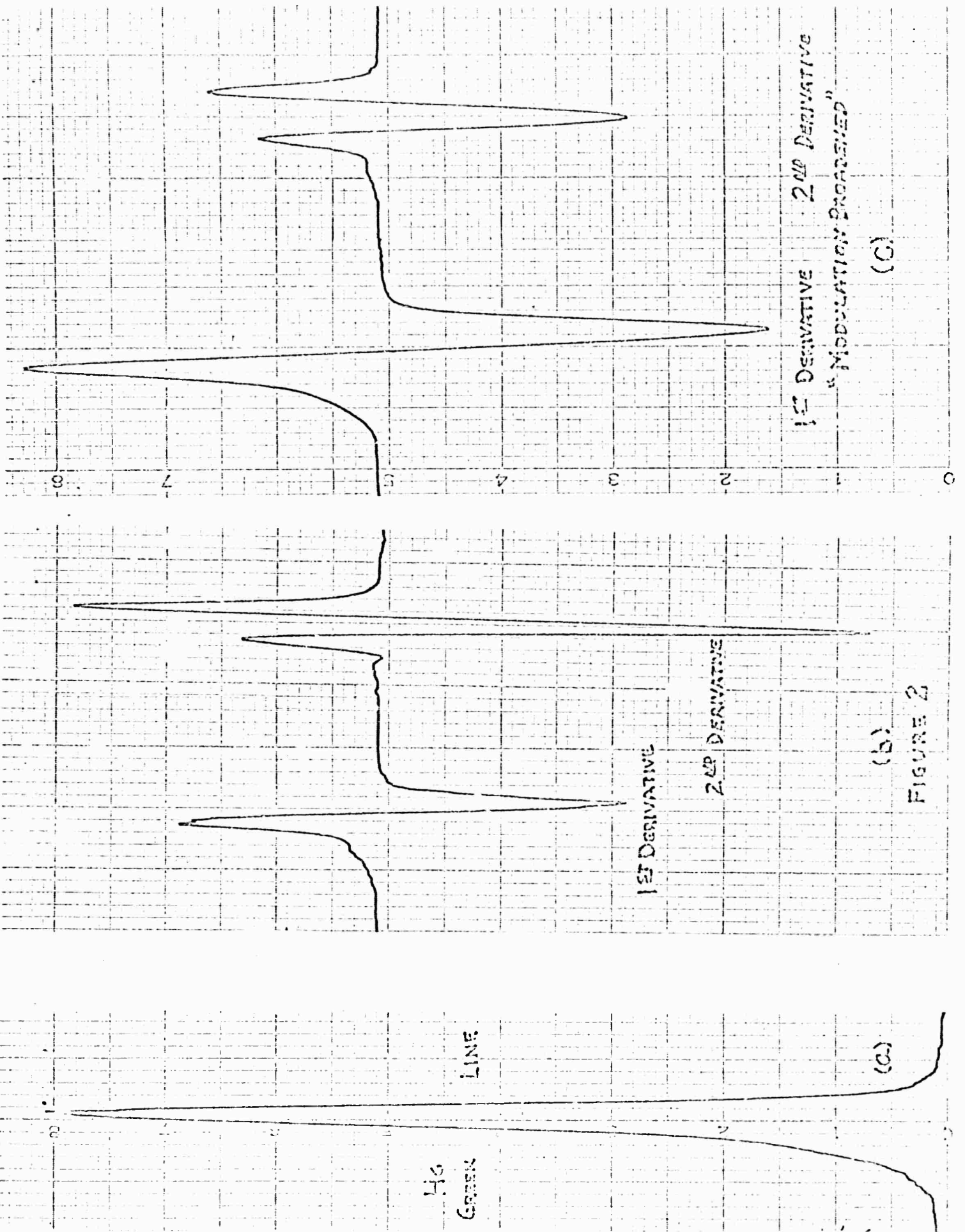


Figure 1



(a)

(b)

(c)

FIGURE 2

DERIVATIVE OF SILICON TRANSMISSION
 REGION OF INDIRECT PHONON TRANSITIONS

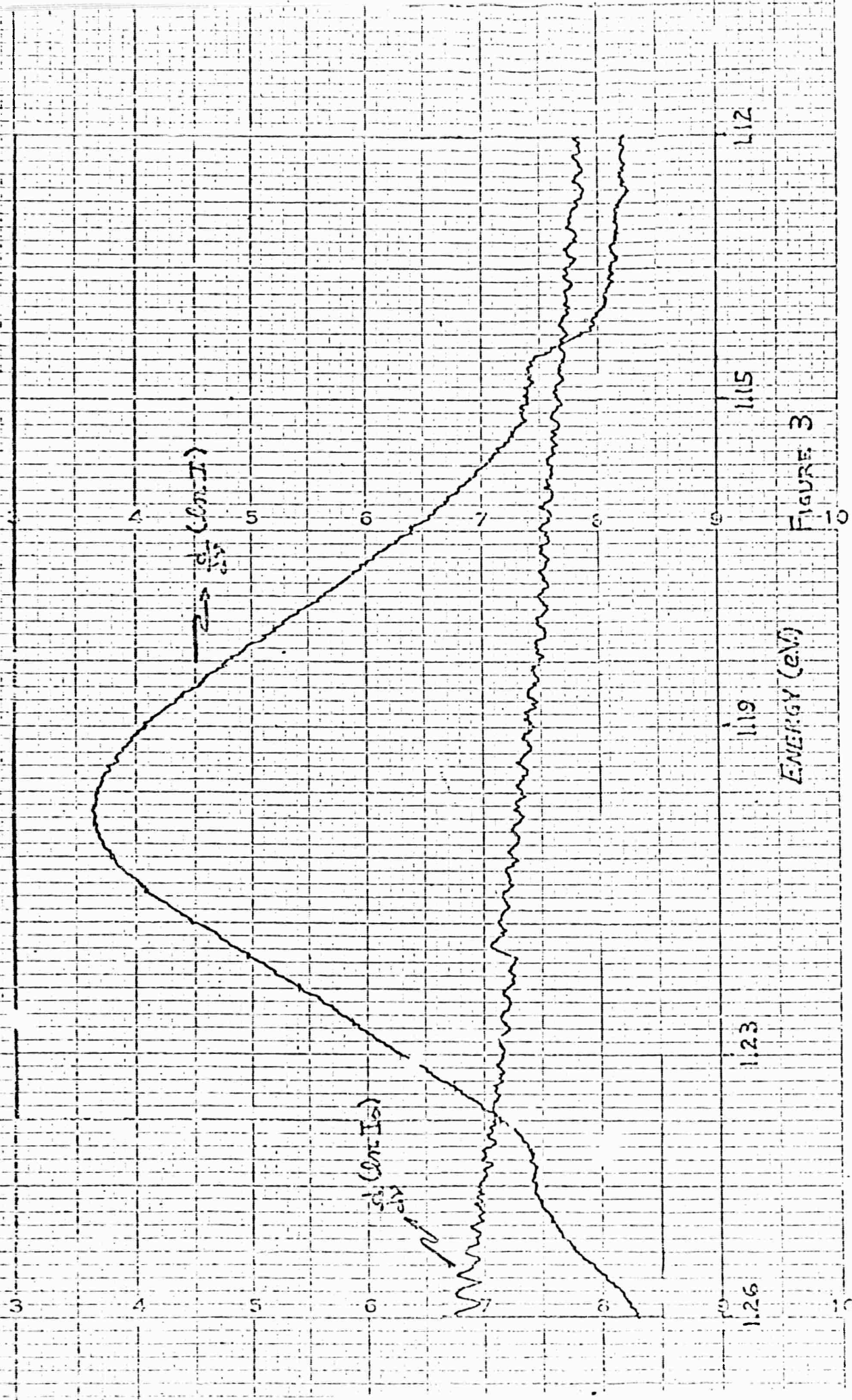


FIGURE 3

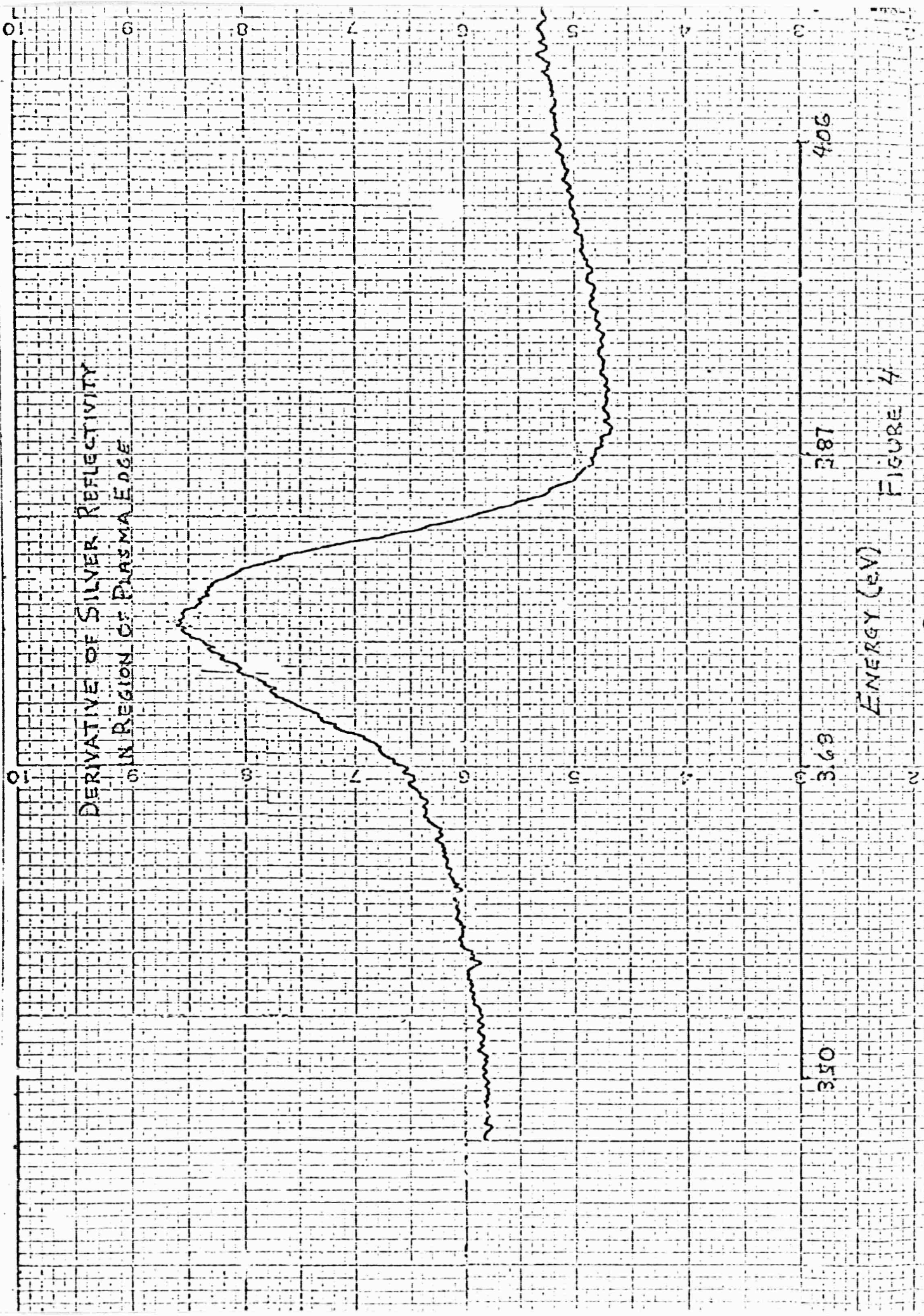


FIGURE 4

He-Ne PLASMA OSCILLATOR AND REGENERATIVE AMPLIFIER

J. P. Biscar, D. Petrac and R. Braunstein

While several Ne-Ne gas lasers were being placed in operation for some Brillouin scattering experiments, plasma oscillations in the frequency range from 200 kHz to 430 kHz were encountered whose frequency could be changed by external conditions. The results of this study were reported in Physics Letters 22, 430 (1966). A copy of this publication will be found in the Appendix.

REFLECTION OF ATOMS FROM STANDING LIGHT WAVES

R. Braunstein (UCLA) in collaboration with S. Aultshuler and
L. M. Frantz (TRW Systems, Redondo Beach, California)

It was shown that it is theoretically possible for neutral atoms to undergo Bragg reflection from standing light waves. This phenomena is analogous to ordinary scattering of light waves by periodic structures such as diffraction gratings and crystals. A note on this calculation was published in Phys. Rev. Letters 17, 231 (1966); a copy of this publication will be found in the Appendix.

The above calculations showed that a neutral particle will be deflected through twice the Bragg angle given by $h\omega/Mv$ where ω is the frequency of the standing light wave and M and v are the mass and velocity of the scattered neutral particle. If this condition is not satisfied, there is essentially no scattering. If a neutral atom of mass 20 and kinetic energy 1 ev is incident within a ruby laser cavity, the angle of deflection will be of the order of 10^{-5} radians. Although it is experimentally feasible to measure such deflection angles, much larger angles will be obtained if sub-thermal beams could be employed. Various experimental designs are being considered to ascertain the feasibility of performing such neutral atom deflection experiments. This work is being done in collaboration with S. Aultshuler and L. M. Frantz of TRW Systems, Redondo Beach, California.

APPENDIX

Saturable Transmission by Multiphoton Absorption in Semiconductors*

R. Braunstein

Department of Physics

University of California at Los Angeles, California

Multiphoton absorption can set an intrinsic upper limit to the power density transmittable through semiconductors. This mechanism is an effective means of optically pumping semiconductor lasers, can limit the power density from such devices, or can enable the fashioning of nonlinear optical power limiters.

*This research is part of Project Defender Contract NONR 233(93) from the Office of Naval Research, the Advanced Project Agency and the Department of Defense of the United States of America.

Recent measurements of double-photon absorption in a number of semiconductors such as CdS,^{1,2} GaAs,³ PbTe,^{4,5} and InSb⁴ have shown that the theory^{1,6} developed for the two-photon excitation of interband transitions is adequate to account for the observed cross-sections. It is of some interest, because of this agreement between theory and experiment for the above semiconductors, to consider the calculation of the double-photon absorption for all the III-V compounds since such multiphoton processes can set an intrinsic upper limit to the flux density that can be transmitted through such media using presently available laser sources. Since the absorption coefficient for this process obeys a nonlinear transmission law, the multiphoton absorption mechanism can serve as an efficient agent for multiphoton optical pumping of semiconductor lasers,^{3,5,7} set an intrinsic upper limit to the power density obtainable from semiconductor lasers, or enable one to fashion nonlinear optical power limiters.

The previous theory,^{1,6} developed for the double-photon absorption in semiconductors utilized a three-band model for the band structure and took account of the parity of the vertical transitions. However, the application of this theory to allowed-forbidden two photon absorption in a two band model, reveals simple generalizations regarding the underlying band parameters which determine the cross-section for all the III-V-II-VI compounds and so enables one to succinctly set a lower bound for this cross section for this class of materials. Using the framework of the theory^{1,6}, it can be easily shown that the double photon absorption coefficient for a two-band model is given by:

$$K_2 = \frac{(2)^{3/2} \pi N_2 \alpha_c^2 |Pvc|^2 e^4}{c n_1 n_2^2 m^{3/2} (\alpha_c + \alpha_v)^{5/2}} [\hbar\omega_1 + \hbar\omega_2 - E_g]^{3/2} \left[\frac{1}{\hbar\omega_1} + \frac{1}{\hbar\omega_2} \right]^2 \quad (1)$$

where $\hbar\omega_1$ and $\hbar\omega_2$ are the photon energies, n_1 and n_2 are the indices of refraction for photon one and two respectively, E_g is the energy gap, α_c and α_v are the inverse effective masses of the conduction and valence bands, and $|Pvc|^2$ is the square of the momentum matrix element for the inter-band transition. This expression is essentially similar to that previously obtained¹ using the three-band model, with the simplification that only one matrix element, the inter-band matrix element remains to be specified since we have performed the integration over the intra-band matrix element of zeroth order in \vec{k} which vanishes at an extreme and is equal to the group velocity times the free electron mass.⁸

In order to evaluate the above expression for a specific substance, a knowledge of α_c , α_v , E_g and $|Pvc|^2$ is necessary. However, it can be shown, using $\vec{k} \cdot \vec{p}$ perturbation theory,⁹ that the valence and conduction band effective masses at $\vec{k}=0$ can be accounted for by assuming that $|Pvc|^2$ is a constant¹⁰ for all the III-V compounds and is equal to 11.5 eVm. It is instructive to re-express the absorption coefficient in equation (1) in terms of a nonlinear absorption cross-section; taking the above value for the square of the matrix element and assuming $\hbar\omega_1$ and $\hbar\omega_2$ are approximately equal to E_g , one obtains

$$\sigma_2 = \frac{3.6 \times 10^{-48} \alpha_c^2}{n_1 m_2^2 (\alpha_c + \alpha_v)^{5/2}} \cdot \frac{1}{E_g^{5/2}} \text{ cm}^4 \text{ sec.} \quad (2)$$

The conduction band effective masses for the III-V compounds are given by $\vec{k}\cdot\vec{p}$ theory as

$$\alpha_c = \frac{m}{m_c} = 1 + \frac{2}{3} |P_{V_k, c k}|^2 \left(\frac{2}{E_g} + \frac{1}{E_g + \Delta} \right) \quad (3)$$

where Δ is the spin-orbit splitting at $\vec{k}=0$. Using the experimentally determined values¹⁰ of α_c , E_g , and Δ or the calculated values of α_c from equation (3), and assuming $\alpha_v \approx 1$, explicit values for the double-photon absorption cross-sections from equation (2) can be calculated. The values σ_2 for some representative compounds are shown in Table I. It is seen that σ_2 increases as the band gap decreases. In the derivation of equation (1), it was explicitly assumed that the absorption occurs via a single intermediate state which allows coupling between the initial and final state. In fact, it is necessary to sum over all possible intermediate states; consequently, this calculation represents a lower bound for σ_2 .

Let us now consider the transmission laws obeyed for a medium within which a linear and a quadratic loss process can simultaneously take place. In the steady state, the transmitted flux is given by the continuity equation:

$$\nabla \cdot F = -\sigma_1 F N_1 - \sigma_2 F^2 N_2 \quad (4)$$

where σ_1 , is the linear absorption cross-section in units of cm^2 , σ_2 is the double-photon absorption cross-section in $\text{cm}^4 \text{sec}$, N_1 and N_2 are the density of centers responsible for the single and double-quanta process, respectively, and F is the flux in $\text{photons}/\text{cm}^2/\text{sec}$.

We shall assume that N_1 and N_2 are independent of F , i.e., the lifetime for recombination to the ground state is short compared to duration of the light pulse. For a plain parallel state of thickness r and neglecting reflection losses, the transmission $= F/F_0$ is given for:

$$\text{Plane: } \frac{F}{F_0} = \frac{\sigma_1 N_1 r}{\exp(\sigma_1 N_1 r) [\sigma_1 N_1 r + \sigma_2 N_2 r F_0] - \sigma_2 N_2 r F_0} \quad (5)$$

Similar results can be obtained for spherical and cylindrical geometry where for simplicity we neglect σ_1 in these cases:

$$\text{Spherical: } \frac{F}{F_0} = \frac{1}{\sigma_2 N_2 \frac{r^2}{\Lambda_0^2} F_0 + \frac{r^2}{\Lambda_0^2} - \sigma_2 N_2 r F_0} \quad (6)$$

$$\text{Cylindrical: } \frac{F}{F_0} = \frac{1}{\sigma_2 N_2 r F_0 \ln \Lambda + \frac{r}{\Lambda_0} - \sigma_2 N_2 r F_0 \ln \Lambda_0} \quad (7)$$

It is seen from equations (5), (6), (7), that for high incident intensities the transmission saturates for all geometries:

Figure 1 shows a plot of the absorption $A = 1 - F/F_0$ for the plain geometry for a medium having linear and quadratic loss processes simultaneously present. When the parameter $\sigma_2 N_2 r F_0$, the quadratic loss process becomes dominant and the transmission ultimately saturates, showing that there is an intrinsic upper limit to the power density

that can be transmitted for a multiphoton process. It should be noted that only the linear absorption process yields an exponential fall-off of the intensity with distance, while the quadratic and higher order processes will fall off inversely proportional to the product of the distance and intensity.

It is of interest to consider the regime of intensity where the double-photon process will become dominant in semiconductors. Although semiconductors injection lasers have less power output compared to most optically pumped solid state lasers, they are relatively small area devices so the flux per unit area are still quite high at the emitting junctions. Furthermore, the emitted frequencies lie slightly below the band-gap, satisfying the threshold conditions for double-photon absorption. Considering a GaAs diode of length 0.1 cm and using σ_2 , the intrinsic upper limit to the power output from GaAs should not exceed 10^9 watts/cm²; similar results were obtained for GaAs¹¹ using a theory of Keldysh¹² even if an electron-hole pair created by double-photon absorption subsequently recombines and re-emits a photon, two quanta will be annihilated to produce one subsequently re-emitted quantum. Since $\sigma_2 \sim 1/E_g^{5/2}$, this process will set in at lower power densities for the lower gap materials. Q-switching, in the attempt to yield higher power densities, will not circumvent the double-photon loss mechanism.

The fact that double-photon absorption is proportional to the product of the intensity and length of path in the medium, indicates that it is an effective means of volume generation of electron-hole pairs to induce laser action as opposed to single-quanta pumping of semiconductors

where high generation rates are limited to surface regions of semiconductors as was experimentally demonstrated for CdS⁷, GaAs³, PbTe⁵. The results of the above calculation show that the appropriate semiconductor can also be used as an effective nonlinear optical power limiter.

Although the considerations in this case were directed to the case of double-photon inter-band transitions similar considerations apply to transitions between discrete levels in a solid, gas, or liquid. In the case of the propagation of a laser beam through a gaseous atmosphere, if care is not taken so that no state exists at twice the laser frequency to which double-quanta absorption can take place, there is an intrinsic upper limit to the power density that can be transmitted through such an atmosphere. Although we would normally consider only multiphoton absorption in cases where high intensity lasers are available, the fact that absorption for this process is proportional to the length of path and the intensity, such nonlinearities may manifest themselves in a number of astronomical cases where exceedingly long paths are involved such as the case of a planetary nebula or propagation through inter-stellar hydrogen.

References

1. R. Braunstein and M. Ockman, Phys. Rev. 134, A499 (1964).
2. Paul J. Regensburger and E. Panizza, Phys. Rev. Letters 18, 113 (1967).
3. N. G. Basov, A. Z. Grasyik, I. G. Zubarev, and V. A. Katulin, Zh. Eksperim. i Teor. Fizi - Pis'ma Redakt 1, No. 4, 29 (1965) [translation: JETP Letters 1, 118 (1965)].
4. K. J. Button, Benjamin Lax, Margaret H. Weiler, and M. Reine, Phys. Rev. Letters 17, 1005 (1966).
5. C. K. M. Patel, P. A. Fleury, R. E. Slusher, and H. L. Frisch, Phys. Rev. Letters 16 (1966).
6. R. Braunstein, Phys. Rev. 125, 475 (1962).
7. V. K. Kanyukhov, L. A. Kulevski, and A. M. Prokhorov, Dokl. Akad. Nauk SSSR 164, 1012 (1965) [translation: Soviet Phys. - Doklady 10, 943 (1966)].
8. A. H. Wilson, "The Theory of Metals," (Cambridge University Press, 2nd edition, 1953).
9. E. O. Kane, J. Phys. Chem. Solids 1, 245 (1957).
10. R. Braunstein and E. O. Kane, J. Phys. Chem. Solids 23, 1423 (1962).
11. F. V. Bunkin and A. M. Prokhorov, J. Exptl. Theoret. Phys. (U.S.S.R.) 48, 1084 (1965) [translation: Soviet Phys. - JETP 21, 725 (1965)].
12. L. V. Keldysh, JETP 47, 1945 (1964); Soviet Phys. - JETP 20, 1307 (1965).

Figure Captions

Figure 1. Transmission law for a medium with linear and quadratic losses simultaneously present.

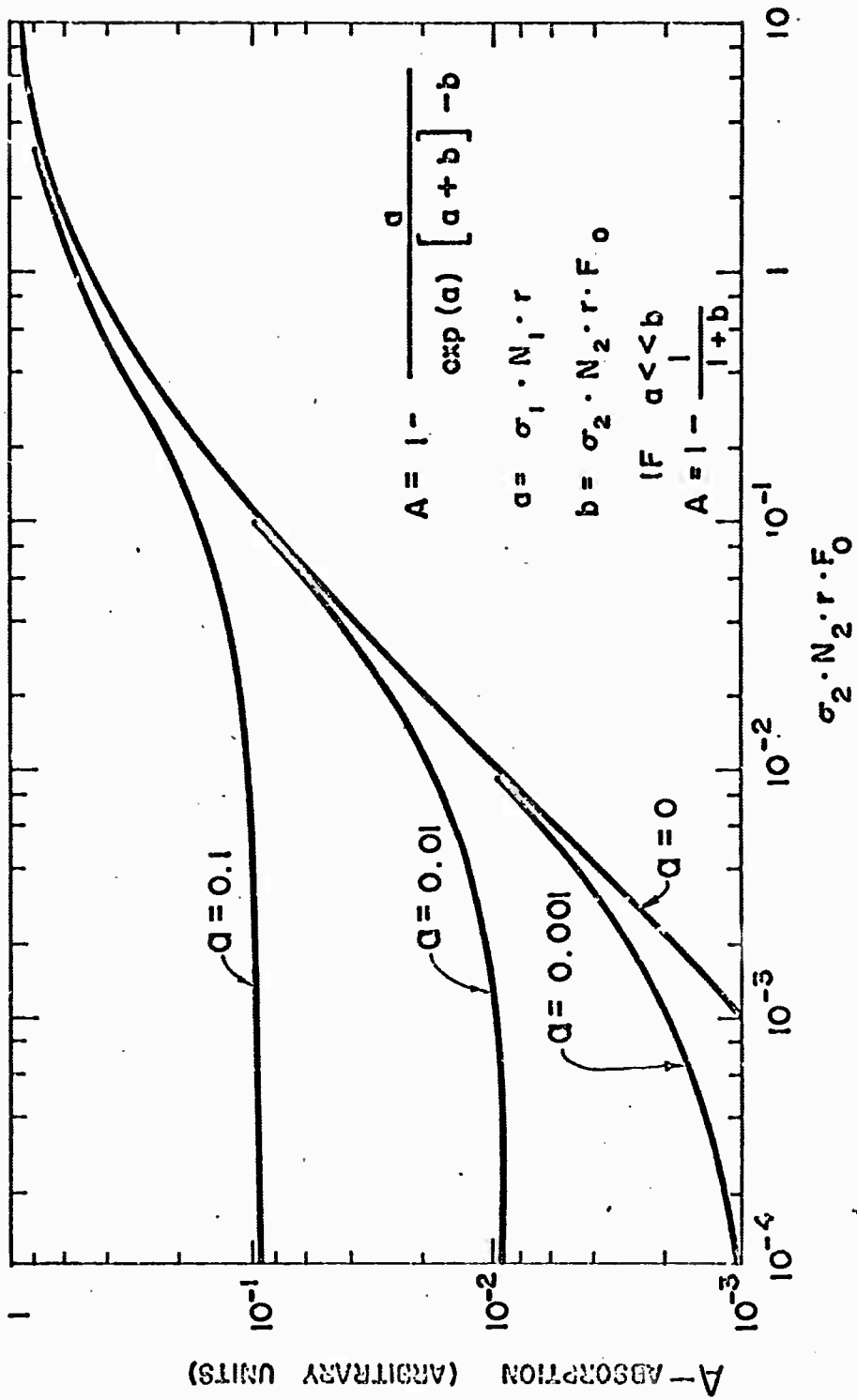


Table I

Band parameters and calculated double-photon absorption cross-sections.

	GoAs	InP	InAs	InSb
$E_g - \text{eV}$	1.53	1.34	0.45	0.25
$a_c -$	13.3	15.2	38.5	65.5
$\Delta -$	0.33	0.24	0.43	0.84
$\sigma_2 - \text{cm}^4 \text{sec}$	2.8×10^{-49}	3.7×10^{-49}	4.0×10^{-48}	1.4×10^{-47}

ERRATUM

He-Ne plasma oscillator and regenerative amplifier,
J. P. Biscar, Physics Letters 22 (1960) 430

The heading of this letter should read:

He-Ne plasma oscillator and regenerative amplifier *

J. P. Biscar †, R. Braunstein and D. Petrac
*Department of Physics, University of California
at Los Angeles, California*

- This research is part of Project Defender Contract Nonr 235(93), from the Office of Naval Research, the Advanced Project Agency, and the Department of Defense of the United States of America.
† C.N.R.S. and NATO Fellow.

case $\nu_0 = 132$ Mc/s. Fig. 1B (5 nsec/div) is a beat display corresponding to ν_0 for the TEM₀₀ transverse mode. (The upper curve 1A is the "dark" display obtained by merely covering the photomultiplier). Fig. 1C (5 nsec/div) is a display of ν_0 and $2\nu_0$ combined, also for the TEM₀₀. The presence of $2\nu_0$ (which is obtained by increasing the driving power level) is an indication of the simultaneous oscillation of at least three longitudinal modes. The frequency response of the photomultiplier falls off around 350 Mc/s. For that reason $3\nu_0$ was not observed. Upon transition to higher transverse modes (i.e. changing $m+n$ in eq. (1) beat frequencies corresponding to $\Delta(m+n) \neq 0$ were observed. Curves D, E, F in fig. 1 are the examples of the displays corresponding to $\nu_0(0+f) = 28$ Mc/s (1D), $\nu_0(1+f) = 160$ Mc/s (1E), $\nu_0(1-f) = 104$ Mc/s (1F). In a first attempt frequencies corresponding to $(0+f)\nu_0$, $(0+2f)\nu_0$, $(1-f)\nu_0$, $(1+0)\nu_0$, $(1-f)\nu_0$, $(2+0)\nu_0$, and $(2+f)\nu_0$ were observed. It should be noted that the various frequencies are obtained as "clean" displays by suitably varying both the driving po-

wer level and the angular position of the concave mirror.

It is noted that in addition to the above frequencies one gets some times the frequencies corresponding to $(1-f)\nu_1$, $(1+0)\nu_1$, $(1+f)\nu_1$, $(2+0)\nu_1$, and $(2+f)\nu_1$ where $\nu_1 = 128$ Mc/s.

The significance and meaning of ν_1 is being studied and a more detailed account of the present research will be published in a forthcoming publication.

The author is indebted to Drs. P.A. Forsyth and R. Mitalas for reading the manuscript and to Mr. W. Heinrich for skillful technical assistance.

This work was supported by grants from NRC and DRB of Canada.

References

1. G.E. Francois, Phys. Rev. 143 (1936) 597.
2. G.D. Boyd and H. Kogelnik, Bell System Tech. J. 41 (1962) 1347.
3. J.P. Goldsborough, Applied Optics 3 (1964) 207.

He-Ne PLASMA OSCILLATOR AND REGENERATIVE AMPLIFIER

J. P. MISCAR

Department of Physics, University of California at Los Angeles,
California

Received 11 July 1966

A new type of gas plasma oscillations is reported, obtained by shunting the plasma with an external capacitor. This configuration can work as an oscillator or as a regenerative amplifier.

This letter reports the conditions and the main data of peculiar plasma oscillations. The frequency and the amplitude of these oscillations depend essentially on the external capacitor connected to the ends of the plasma tube and on the current of the discharge. Many spontaneous oscillations have been reported [1-2] on direct current glow discharges in noble gases, and in the frequency range lower than 50 kHz. As Donahue and Dicke [2] have demonstrated, moving striations are almost always present in d.c. discharge, and they have been studied [3-5]. Ion sound waves in plasmas have been reported too [6-7] and also unexplained waves [8] in r.f. discharge. All of these

former instabilities depend on plasma internal conditions and are also difficult to control whereas in this experiment all the parameters are easily controlled.

The experiment is carried out with a plasma obtained through a d.c. discharge in a tube 60 cm length and 5 mm in diameter. The tube is filled with a 5:1 (by pressure) helium neon gas mixture to a total pressure of 1.22 Torr. A resistor of 60 k Ω is always used as ballast. The plasma oscillations are detected with a very light electrostatic coupling to the plasma of a 10 M Ω probe and are displayed in an oscilloscope.

The plasma obtained under these conditions

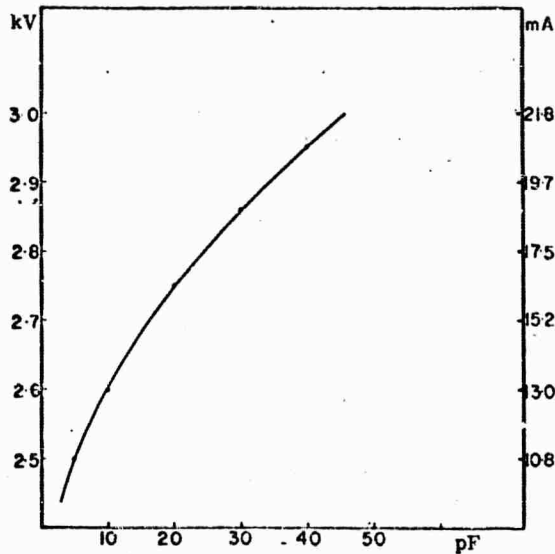


Fig. 1. Current (and voltage) threshold versus external capacitor C.

has a linear negative characteristic between 8 and 22 mA. However, any type of oscillant circuit shunted by this element of negative resistor cannot oscillate, but a simple capacitor for a very precise current is successful. With this configuration, briefly, three different kinds of oscillations are:

- 1) Some instability of frequency lower than 50 KHz, similar to the oscillations reported by Donahue [2].
- 2) With a capacitor $C > 50$ pF, there are strong relaxation oscillations whose frequency changes (100-150 KHz) with the voltage of the power supply, but whose amplitude remains constant.
- 3) The most interesting and completely different oscillations were found with $C < 50$ pF.

The output is always perfectly sinusoidal and, after some thermalisation, is stable in amplitude. The frequency stability is $\Delta f/f \approx 3 \times 10^{-4}$.

An important point, is that, for a given value of the external capacitor, these oscillations start at a very precise voltage or current threshold. For example, using a power supply of 3000 volt, the precision of this threshold is about one volt, demonstrating that the negative characteristic does not explain the mechanism of these plasma instabilities. Fig. 1 shows the variation of this threshold versus the capacitor value.

When you find the threshold, by decreasing the voltage of the power supply the amplitude of these oscillations increases linearly. (They can also produce some output power and if they become too great they can extinguish the plasma). However, the control of their amplitude is made by the set voltage of the power supply.

The frequency also depends on the external conditions. With the same plasma tube one can cover the frequency range from 200 kHz to 430 kHz by changing only external conditions.

At each of these preceding frequencies, this plasma oscillator works as a regenerative amplifier, but only if the set voltage is very close to the threshold voltage. For a difference over 2 V, there is no further amplification; the oscillator is autonomous. We use an electrostatic coupling of the external h.f. generator to the plasma tube (in the opposite side of the output). The set voltage must be adjusted at the beginning of the proper oscillations at the frequency f_0 . By changing the frequency of the external generator, one sees a great maximum for the precise frequency f_0 of the plasma oscillator. It is difficult to know the exact input in the plasma, because of the extremely light coupling. However, a gain superior to 20 dB was found with a band pass of 4 kHz.

A longitudinal magnetic field decreases linearly the amplitude of the oscillations, whereas a transverse magnetic field increases them. The force behind these plasma instabilities is the existence of atoms in metastable state which are also sensitive to a precise near infrared wavelength. In another paper, we will report this optical property with the "plasma mechanism".

References

1. M. J. Druyvesteyn and F. M. Penning, Rev. Mod. Phys. 12 (1940) 87.
2. T. M. Donahue and Dieke, Phys. Rev. 81 (1951) 248.
3. H. S. Robertson, Phys. Rev. 105 (1957) 368.
4. L. Pekarek, Phys. Rev. 108 (1957) 1371.
5. H. S. Robertson and M. A. Hakeem, Proc. Fifth Intern. Conf. on Ionization phenomena in gases, Vol. 1, p. 550.
6. I. Alexeff and R. L. Neidigh, Bull. Amer. Phys. Soc. 6 (1961) 304.
7. I. Alexeff and R. L. Neidigh, Phys. Rev. 129 (1963) 516.
8. Noriyoshi Sato and Yoshisuke Hatta, Phys. Rev. Letters 16 (1966) 306.

* * * * *

REFLECTION OF ATOMS FROM STANDING LIGHT WAVES

S. Altshuler and L. M. Frantz
TRW Systems, Redondo Beach, California

and

R. Braunstein
University of California, Los Angeles, California
(Received 16 May 1966)

It was predicted in 1933 by Dirac and Kapitza¹ that electrons could undergo Bragg reflection from standing light waves. This phenomenon of electron-wave scattering is analogous to the ordinary scattering of light waves by periodic structures such as diffraction gratings and crystals. Recent interest² has been stimulated by the increased possibility of observing the effect using the intense light beams now available as a result of laser technology.

We wish to point out that Bragg reflection by standing light waves is not restricted to elec-

trons, but should occur for all particles capable of scattering photons, including neutral atoms. The Dirac-Kapitza analysis results in the expression for the scattering probability per unit length k of the electron traversing the region occupied by the standing waves,

$$k = \frac{4\pi^2 n^2 c^4}{\omega^2 \gamma v} \frac{d\sigma(\pi)}{d\Omega}, \tag{1}$$

where n is the photon number density, ω is the angular frequency, γ is the spectral width of the electromagnetic radiation, v is the electron

velocity, and $d\sigma(\pi)/d\Omega$ is the Thomson differential cross section for backscatter of a photon by a free electron. Although the original analysis and all of the subsequent references have been concerned explicitly with electrons, it is of considerable interest to note that the same analysis applies regardless of the nature of the incident particle. Equation (1) remains valid provided only that $d\sigma(\pi)/d\Omega$ be interpreted as the differential cross section for backscatter of a photon from the particle in question.

Dirac and Kapitza regard the standing wave as a superposition of two traveling waves. The essence of their analysis is then the computation of the stimulated backscatter rate, viz., that corresponding to scattering a traveling-wave photon from a mode associated with one propagation direction into the mode associated with the opposite direction. Because photons obey Bose statistics, this rate is proportional not only to the radiation density in the mode from which the photon is absorbed, but also to the radiation density in the mode into which the photon is emitted.³ It is to be emphasized, however, that this proportionality to the photon density in the final-state mode is a consequence of only the Bose statistics obeyed by the photons, and is independent of the nature of the scatterer. It is for this reason that the Dirac-Kapitza analysis is directly generalizable from electrons to arbitrary scatterers.

Equation (1) applies only if the Bragg condition is satisfied, i.e., the particle must be incident at an angle θ_B relative to the direction normal to the photon-propagation vector. The Bragg angle is given by $\theta_B = \hbar\omega/Mcv$, where M is the particle mass. The particle is deflected through an angle $2\theta_B$; however, if the Bragg condition is not satisfied, there is essentially no scattering.

As an illustration of the magnitude of the effects, let us consider the scattering of a neutral atom of atomic mass of about 20 and kinetic energy of 1 eV. We shall choose the radiation frequency to be that appropriate to a ruby laser ($\omega = \pi \times 10^{15}$ sec⁻¹), a power density

of one megawatt per cm², and a typical cavity loss rate γ of 10^7 sec⁻¹. For the back-scattering cross section, $d\sigma(\pi)/d\Omega$, we choose a typical value of 10^{-28} cm² corresponding to Rayleigh scattering. It should be observed, however, that $d\sigma/d\Omega$ for atoms is strongly frequency dependent, and at or near resonances can be many orders of magnitude larger than the value for Rayleigh scattering. For the numbers we have chosen, the deflection angle is quite small, namely, $2\theta_B = 2 \times 10^{-5}$ rad. However, the interaction is quite strong; the scattering probability per unit length is $k = 6.2$ cm⁻¹, and, as we have just indicated, it can be enormously greater near a resonance. This strong interaction suggests that a large net scattering angle may be attainable with a succession of individual Bragg scatterings by an appropriate arrangement of successive standing-wave cavity orientations.

Finally, it should be mentioned that the above reasoning can be readily extended to multiple-photon events. That is, to every N -photon scattering process occurring in free space there corresponds an N -photon stimulated scattering process for which the Bragg angle is $N\hbar\omega/Mcv$, the scattering angle is $2N\hbar\omega/Mcv$, and the scattering probability per unit length is proportional to the $2N$ th power of the photon density n^{2N} .

¹P. L. Kapitza and P. A. M. Dirac, Proc. Cambridge, Phil. Soc. **29**, 297 (1933).

²A. C. Hall, Nature **199**, 683 (1963); I. R. Gatland, L. Gold, and J. W. Moffatt, Phys. Letters **12**, 105 (1964); L. S. Bartell, H. Bradford Thompson, and R. R. Roskos, Phys. Rev. Letters **14**, 851 (1965); J. H. Eberly, Phys. Rev. Letters **15**, 91 (1965); H. Schwartz, H. A. Tourtelotte, and W. W. Garrett, Bull. Am. Phys. Soc. **10**, 1129 (1965); L. S. Bartell and H. Bradford Thompson, *Physics of Quantum Electronics*, edited by P. L. Kelley, B. Lax, and P. E. Tannenwald (McGraw-Hill Book Company, Inc., New York, 1966), p. 129; H. Schwartz, in Proceedings of the International Conference on Quantum Electronics, Phoenix, April 1966 (unpublished), post deadline paper.

³P. A. M. Dirac, *Quantum Mechanics* (Oxford University Press, London, 1947), 3rd ed., Chap. 10, p. 232.

DOCUMENT CONTROL DATA - R & D

(Security classification of title, body of abstract and indexing annotation must be entered when the overall report is classified)

1. ORIGINATING ACTIVITY (Corporate author) University of California Department of Physics Los Angeles, California		2a. REPORT SECURITY CLASSIFICATION Unclassified	
		2b. GROUP N/A	
3. REPORT TITLE "Study of Optical Interactions in Solids"			
4. DESCRIPTIVE NOTES (Type of report and inclusive dates) Semiannual Technical Report (For Period 21 March 1968)			
5. AUTHOR(S) (First name, middle initial, last name) Braunstein, R. - Professor Biscar, J. P. Gratch, S. Welkowsky, M.			
6. REPORT DATE May 1968		7a. TOTAL NO. OF PAGES 67	7b. NO. OF REFS 27
8a. CONTRACT OR GRANT NO. NONR-233(93)		9a. ORIGINATOR'S REPORT NUMBER(S)	
b. PROJECT NO. ARPA #306		9b. OTHER REPORT NO(S) (Any other numbers that may be assigned this report)	
c.			
d.			
10. DISTRIBUTION STATEMENT Qualified requesters may obtain copies of this report from DDC.			
11. SUPPLEMENTARY NOTES		12. SPONSORING MILITARY ACTIVITY Physical Sciences Division Office of Naval Research Washington, D. C. 20360	
13. ABSTRACT Multiphoton absorption in semiconductors was investigated with emphasis on the III-V compounds. It was shown that this mechanism can set an intrinsic upper limit to the power density transmittible through semiconductors. This mechanism is an effective means of optically pumping semiconductor lasers, can limit the power density obtainable from such devices, or can enable the fashioning of nonlinear optical elements. Laser action in a large volume of Ga As was excited by double-photon pumping using a Q-switched neodymium laser, yielding output power of the order of a megawatt/cm ² at 8365 Å at liquid nitrogen temperature. A new temperature anomaly of the threshold for stimulated Raman emission in liquid benzene was discovered and investigated. This effect indicates that self-focusing of the exciting laser beam does not explain previously observed Raman thresholds.			

14 KEY WORDS	LINK A		LINK B		LINK C	
	ROLE	WT	ROLE	WT	ROLE	WT
Laser Raman scattering Nonlinear optics Semiconductors Optical derivative spectroscopy						